The dimer model in statistical mechanics

Béatrice de Tilière [1]

September 11, 2014

[1]Laboratoire de Probabilités et Modèles Aléatoires, Université Pierre et Marie Curie, 4 place Jussieu, F-75005 Paris. beatrice.de_tiliere@upmc.fr. These notes were written in part while at Institut de Mathématiques, Université de Neuchâtel, Rue Emile-Argand 11, CH-2007 Neuchâtel. Supported in part by the Swiss National Foundation grant 200020-120218.

Contents

Chapter 1

Introduction

1.1 Statistical mechanics and 2-dimensional models

Statistical mechanics is the application of *probability theory*, which includes mathematical tools for dealing with large populations, to the field of *mechanics*, which is concerned with the motion of particles or objects when subjected to a force. Statistical mechanics provides a framework for relating the microscopic properties of individual atoms and molecules to the macroscopic bulk properties of materials that can be observed in everyday life (source: 'Wikipedia').

In other words, statistical mechanics aims at studying large scale properties of physics system, based on probabilistic models describing microscopic interactions between components of the system. Statistical mechanics is also known as *statistical physics*.

It is a priori natural to introduce 3-dimensional graphs in order to accurately model the molecular structure of a material as for example a piece of iron, a porous material or water. Since the 3-dimensional version of many models turns out to be hardly tractable, much effort has been put into the study of their 2-dimensional counterpart. The latter have been shown to exhibit rich, complex and fascinating behaviors. Here are a few examples.

- *Percolation.* This model describes the flow of a liquid through a porous material. The system considered is a square grid representing the molecular structure of the material. Each bond of the grid is either "open" with probability p, or "closed" with probability $1-p$, and bonds are assumed to behave independently from each other. The set of open bonds in a given configuration represents the part of the material wetted by the liquid, and the main issue addressed is the existence and properties of infinite clusters of open edges. The behavior of the system depends on the parameter p: when $p = 0$, all edges are closed, there is no infinite cluster and the liquid cannot flow through the material; when $p = 1$, all edges are open and there is a unique infinite cluster filling the whole grid. One can show that there is a specific value of the parameter p, known as *critical* p, equal to $1/2$ for the square grid, below which the probability of having an infinite cluster of open edges is 0, and above which the probability of it existing and being unique is 1. One says that the system undergoes a *phase transition* at $p = 1/2$. References [Kes82, Gri99, BR06, W$^+$07, Wer09] are books or lecture notes giving an overview of percolation theory.

- The *Ising model.* The system considered is a magnet made of particles restricted to stay on a grid. Each particle has a spin which points either "up" or "down" (spin ± 1). Each configuration σ of spins on the whole grid has an energy $\mathcal{E}(\sigma)$, which is the sum of an interaction

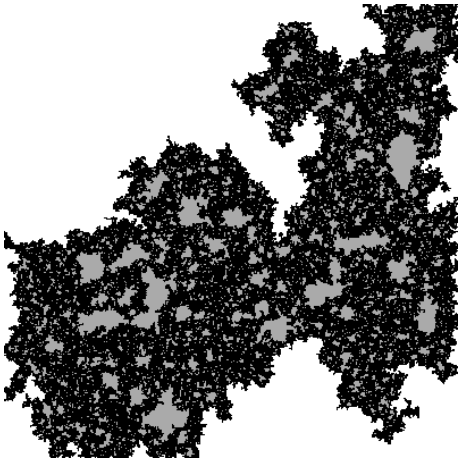

Figure 1.1: An infinite cluster of open edges, when $p = \frac{1}{2}$. Courtesy of V. Beffara.

energy between pairs of neighboring spins, and of an interaction energy of spins with an external magnetic field. The probability of a configuration σ is proportional to $e^{-\frac{1}{kT}\mathcal{E}(\sigma)}$, where k is the Boltzmann constant, and T is the external temperature. When there is no magnetic field and the temperature is close to 0, spins tend to align with their neighbors and a typical configuration consists of all $+1$ or all -1. When the temperature is very high, all configurations have the same probability of occurring and a typical configuration consists of a mixture of $+1$ and -1. Again, there is a *critical temperature* T_c at which the Ising model undergoes a phase transition between the ordered and disordered phase. The literature on the Ising model is huge, as an introductory reading we would suggest the book by Baxter [Bax89], the one by McCoy and Wu [MW73], the lecture notes by Velenik [Vel] and references therein.

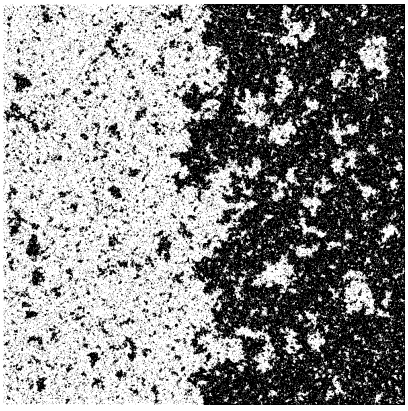

Figure 1.2: An Ising configuration, when $\frac{1}{T} = 0.9$. Courtesy of V. Beffara.

These two examples illustrate some of the principal challenges of 2-dimensional statistical mechanics, which are:

- Find the critical parameters of the models.
- Understand the behavior of the model in the sub-critical and super-critical regimes.

- Understand the behavior of the system at criticality. Critical systems exhibit surprising features, and are believed to be universal in the scaling limit, *i.e.* independent of the specific features of the lattice on which the model is defined. Very precise predictions were established by physicists in the last 30-50 years, in particular by Nienhuis, Cardy, Duplantier and many others. On the mathematics side, a huge step forward was the introduction of the Schramm-Loewner evolution by Schramm in [Sch00], a process conjectured to describe the limiting behavior of well chosen observables of critical models. Many of these conjectures were solved in the following years, in particular by Lawler, Schramm, Werner [LSW04] and Smirnov [Smi10], Chelkak-Smirnov [CS12]. The importance of these results was acknowledged with the two Fields medals awarded to Werner (2006) and Smirnov (2010). Interesting collaborations between the physics and mathematics communities are emerging, with for example the work of Duplantier and Sheffield [DS11].

The general framework for statistical mechanics is the following. Consider an object G (most often a graph) representing the physical system, and define all possible configurations of the system. To every configuration σ, assign an energy $\mathcal{E}(\sigma)$, then the probability of occurrence of the configuration σ is given by the *Boltzmann* measure μ:

$$\mu(\sigma) = \frac{e^{-\mathcal{E}(\sigma)}}{Z(\mathsf{G})}.$$

Note that the energy is often multiplied by a parameter representing the inverse external temperature. The denominator $Z(\mathsf{G})$ is the normalizing constant, known as the *partition function*:

$$Z(\mathsf{G}) = \sum_{\sigma} e^{-\mathcal{E}(\sigma)}.$$

When the system is infinite, the above definition does not hold, but we do not want to enter into these considerations here.

The partition function is one of the key objects of statistical mechanics. Indeed it encodes much of the macroscopic behavior of the system. Hence, its computation is the first question one addresses when studying such a model. It turns out that there are very few models where this computation can be done exactly. Having a closed form for the partition function opens the way to finding many exact results, and to having a very deep understanding of the macroscopic behavior of the system.

Two famous examples are the 2-dimensional Ising model, where the computation of the partition function is due to Onsager [Ons44], and the *dimer model* where it is due to Kasteleyn [Kas61, Kas67], and independently to Temperley and Fisher [TF61]. The dimer model is the main topic of these lectures and is defined in the next section.

1.2 The dimer model

The dimer model was introduced in the physics and chemists communities to represent the adsorption of di-atomic molecules on the surface of a crystal. It is part of a larger family of models describing the adsorption of molecules of different sizes on a lattice. It was first mentioned in a paper by Fowler and Rushbrooke [FR37] in 1937. As mentioned in the previous section, the first major breakthrough in the study of the dimer model is the computation of the partition function by Kasteleyn [Kas61, Kas67] and independently by Temperley and Fisher [TF61].

It is interesting to observe that for a long time, the physics and mathematics communities were unaware of their respective advances. Mathematicians studied related questions as for example

the enumeration of non-intersecting lattice paths by Mac Mahon [Mac01], the understanding of geometric and combinatorial properties of tilings of regions of the plane by dominoes or rhombi. To the best of our knowledge, the latter problem was first introduced in a paper by David and Tomei [DT89]. A major breakthrough was achieved in the paper [Thu90] Thurston, where the author interprets rhombus tilings as 2-dimensional interfaces in a 3-dimensional space. An example of rhombus tiling is given in Figure 1.3.

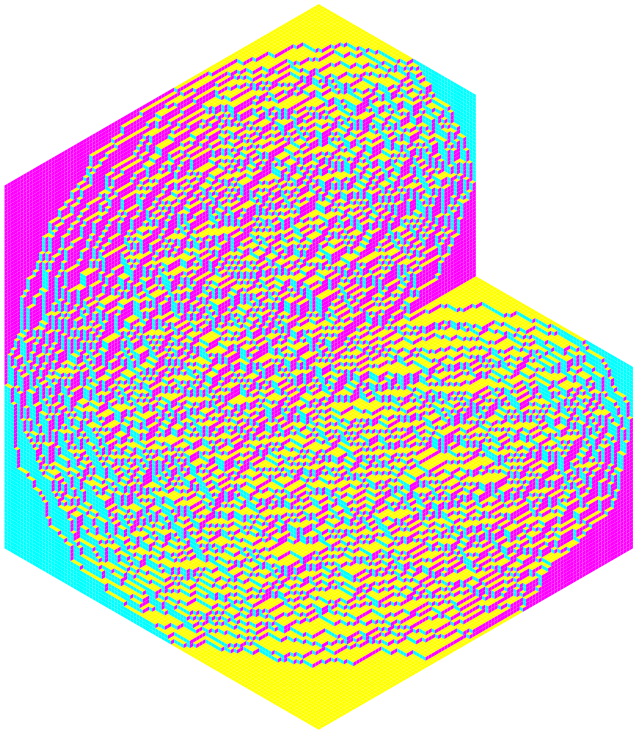

Figure 1.3: Rhombus tiling. Courtesy of R. Kenyon.

In the late 90's and early 00's, a lot of progresses were made in understanding the model, see the papers of Kenyon [Ken97, Ken00], Cohn-Kenyon-Propp [CKP01], Kuperberg [Kup98], Kenyon-Propp-Wilson [KPW00]. In 2006 Kenyon-Okounkov-Sheffield [KOS06], followed by Kenyon-Okounkov [KO06, KO07] wrote breakthrough papers, which give a full understanding of the model on infinite, periodic, bipartite graphs. Such deep understanding of phenomena is a real treasure in statistical mechanics.

My goal for these lectures is to present the results of Kasteleyn, Temperley and Fisher, of Thurston, and of the paper of Kenyon, Okounkov and Sheffield. As you will see, the dimer model has ramifications to many fields of mathematics: probability, geometry, combinatorics, analysis, algebraic geometry. I will try to be as thorough as possible, but of course some results addressing the field of algebraic geometry reach the limit of my knowledge, so that I will only

state them. In other cases, I will try and give ideas of proofs at least.

Inspiration for these notes comes in large parts from the lectures given by R. Kenyon on the subject [Ken04, Ken]. The main other references are [Kas67, Thu90, KOS06, KO06].

Chapter 2

Definitions and founding results

2.1 Dimer model and tiling model

In this section, we define the *dimer model* and the equivalent *tiling model*, using the terminology of statistical mechanics. The *system* considered is a graph $\mathsf{G} = (\mathsf{V}, \mathsf{E})$ satisfying the following: it is planar, simple (no loops and no multiple edges), finite or infinite.

Configurations of the system are perfect matchings of the graph G. A *perfect matching* is a subset of edges which covers each vertex exactly once. In the physics literature, perfect matchings are also referred to as *dimer configurations*, a *dimer* being a di-atomic molecule represented by an edge of the perfect matching. Let us denote by $\mathcal{M}(\mathsf{G})$ the set of all dimer configurations of the graph G.

Figure 2.1 gives an example of a dimer configuration when the graph G is a finite subgraph of the honeycomb lattice $\mathbb{H}$.

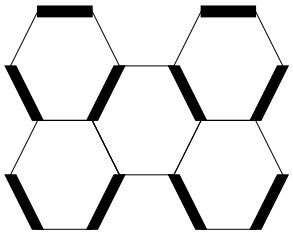

Figure 2.1: Dimer configuration of a subgraph of the honeycomb lattice.

In order to define the equivalent *tiling model*, we consider a planar embedding of the graph G, and suppose that it is *simply connected*, *i.e.* that it is the one-skeleton of a simply connected union of faces. From now on, when we speak of a planar graph G, we actually mean a graph with a particular planar embedding.

The *tiling model* is defined on the dual graph G^* of G. An embedding of the dual graph G^* is obtained by assigning a vertex to every face of G and joining two vertices of G^* by an edge if and only if the corresponding faces of G are adjacent. The dual graph will also be thought of as an embedded graph. When the graph is finite, we take a slightly different definition of the dual: we take G to be the dual of G^* and remove the vertex corresponding to the outer face, as well as edges connected to it, see Figure 2.2.

A *tile* of G^* is a polygon consisting of two adjacent inner faces of G^* glued together. A *tiling* of G^* is a covering of the graph G^* with tiles, such that there are no holes and no overlaps.

Figure 2.2 gives an example of a tiling of a finite subgraph of the triangular lattice $\mathbb{T}$, the dual graph of the honeycomb lattice. Tiles of the triangular lattice are 60°-rhombi, and are also known as *lozenges* or *calissons*.

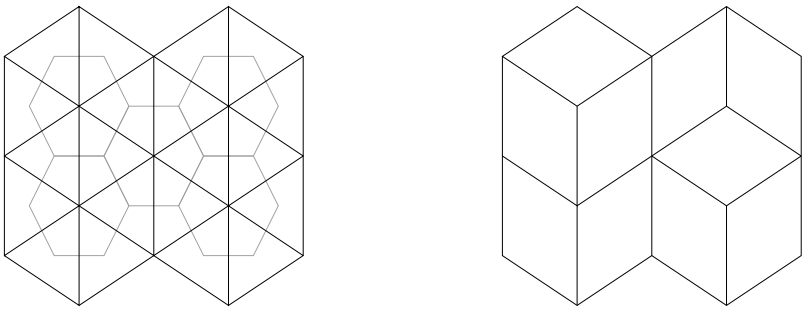

Figure 2.2: Dual graph of a finite subgraph of the honeycomb lattice (left). Tiling of this subgraph (right).

Another classical example is the tiling model on the graph $\mathbb{Z}^2$, the dual of the graph $\mathbb{Z}^2$. Tiles are made of two adjacent squares, and are known as *dominoes*.

Dimer configurations of the graph G are in bijection with tilings of the graph G^* through the following correspondence, see also Figure 2.3: dimer edges of perfect matchings connect pairs of adjacent faces forming tiles of the tiling. It is an easy exercise to prove that this indeed defines a bijection.

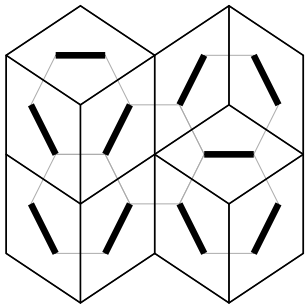

Figure 2.3: Bijection between dimer configurations of the graph G and tilings of the graph G^*.

2.2 Energy of configurations and Boltzmann measure

We let G be a planar, simple graph. In this section, and for the remainder of Chapter 2, we take G to be finite. Suppose that edges are assigned a positive *weight function* ν, that is every edge e of G has weight $\nu(\mathsf{e})$.

The *energy* of a dimer configuration M of G, is $\mathcal{E}(M) = -\sum_{\mathsf{e}\in M} \log \nu(\mathsf{e})$. The *weight* $\nu(M)$ of a dimer configuration M of G, is exponential of minus its energy:

$$\nu(M) = e^{-\mathcal{E}(M)} = \prod_{\mathsf{e}\in M} \nu(\mathsf{e}).$$

Note that by the correspondence between dimer configurations and tilings, the function ν can be seen as weighting tiles of G^*, $\nu(M)$ is then the weight of the tiling corresponding to M.

Weights of configurations allow to introduce randomness in the model: the *Boltzmann measure* μ is a probability measure on the set of dimer configurations $\mathcal{M}(\mathsf{G})$, defined by:

$$\forall\, M \in \mathcal{M}(\mathsf{G}), \quad \mu(M) = \frac{e^{-\mathcal{E}(M)}}{Z(\mathsf{G})} = \frac{\nu(M)}{Z(\mathsf{G})}.$$

The term $Z(\mathsf{G})$ is the normalizing constant known as the *partition function*. It is the weighted sum of dimer configurations, that is,

$$Z(\mathsf{G}) = \sum_{M \in \mathcal{M}(\mathsf{G})} \nu(M).$$

When $\nu \equiv 1$, the partition function counts the number of dimer configurations of the graph G, or equivalently the number of tilings of the graph G^*, and the Boltzmann measure is simply the uniform measure on the set of dimer configurations.

When analyzing a model of statistical mechanics, the first question addressed is that of computing the *free energy*, which is minus the exponential growth rate of the partition function, as the size of the graph increases. The most natural way of attaining this goal, if the model permits, is to obtain an explicit expression for the partition function. Recall that the dimer model is one of the rare 2-dimensional models where a closed formula can be obtained. This is the topic of the next section.

2.3 Explicit computations

The explicit computation of the partition function is due to Kasteleyn [Kas61, Kas67] and independently to Temperley and Fisher [TF61]. A proof of this result is provided in Section 2.3.1, in the case where the underlying graph G is bipartite. This is one of the founding results of the dimer model, paving the way to obtaining other explicit expressions as for example Kenyon's closed formula for the Boltzmann measure [Ken97], see Section 2.3.2. In Section 2.3.3, we provide an example of computation of the partition function and of the Boltzmann measure.

2.3.1 Partition function formula

We restrict ourselves to the case where the graph G is bipartite, the proof in the non-bipartite case is similar in spirit although a little more involved. The simplification in the bipartite case is due to Percus [Per69].

A graph $\mathsf{G} = (\mathsf{V}, \mathsf{E})$ is *bipartite* if the set of vertices V can be split into two subsets $\mathsf{W} \cup \mathsf{B}$, where W denotes white vertices, B black ones, and vertices in W are only adjacent to vertices in B. We suppose that $|\mathsf{W}| = |\mathsf{B}| = n$, for otherwise there are no perfect matchings of the graph G; indeed a dimer edge always covers a black and a white vertex.

Label the white vertices $\mathsf{w}_1, \dots, \mathsf{w}_n$ and the black ones $\mathsf{b}_1, \dots, \mathsf{b}_n$, and suppose that edges of G are oriented. The choice of orientation will be specified later in the proof. Then the corresponding *oriented, weighted, adjacency matrix* is the $n \times n$ matrix K whose lines are indexed by white vertices, whose columns are indexed by black ones, and whose entry $K(\mathsf{w}_i, \mathsf{b}_j)$ is:

$$K(\mathsf{w}_i, \mathsf{b}_j) = \begin{cases} \nu(\mathsf{w}_i\mathsf{b}_j) & \text{if } \mathsf{w}_i \sim \mathsf{b}_j, \text{ and } \mathsf{w}_i \to \mathsf{b}_j \\ -\nu(\mathsf{w}_i\mathsf{b}_j) & \text{if } \mathsf{w}_i \sim \mathsf{b}_j, \text{ and } \mathsf{w}_i \leftarrow \mathsf{b}_j \\ 0 & \text{if the vertices } \mathsf{w}_i \text{ and } \mathsf{b}_j \text{ are not adjacent.} \end{cases}$$

By definition, the determinant of the matrix K is:

$$\det(K) = \sum_{\sigma \in \mathcal{S}_n} \operatorname{sgn}(\sigma) K(\mathsf{w}_1, \mathsf{b}_{\sigma(1)}) \dots K(\mathsf{w}_n, \mathsf{b}_{\sigma(n)}),$$

where $\mathcal{S}_n$ is the set of permutations of n elements. Let us first observe that each non-zero term in the expansion of $\det(K)$ corresponds to the weight of a dimer configuration, up to sign. Thus, the determinant of K seems to be the appropriate object for computing the partition function, the only problem being that not all terms may be counted with the same sign. Note that reversing the orientation of an edge $\mathsf{w}_i\mathsf{b}_j$ changes the sign of $K(\mathsf{w}_i, \mathsf{b}_j)$. The remainder of the proof consists in choosing an orientation of the edges of G allowing to compensate signature of permutations, so that all terms in the expansion of the determinant of K indeed have the same sign.

Let M_1 and M_2 be two perfect matchings of G drawn one on top of the other. Define an *alternating cycle* to be a cycle of G whose edges alternate between edges of M_1 and M_2. Then, an alternating cycle has even length, and if the length is equal to 2, the cycle is a *doubled edge*, that is an edge covered by both M_1 and M_2. The superimposition of M_1 and M_2 is a union of disjoint alternating cycles, see Figure 2.4. This is because, by definition of a perfect matching, each vertex is adjacent to exactly one edge of the matching, so that in the superimposition of two matchings M_1 and M_2, each vertex is adjacent to exactly one edge of M_1 and one edge of M_2.

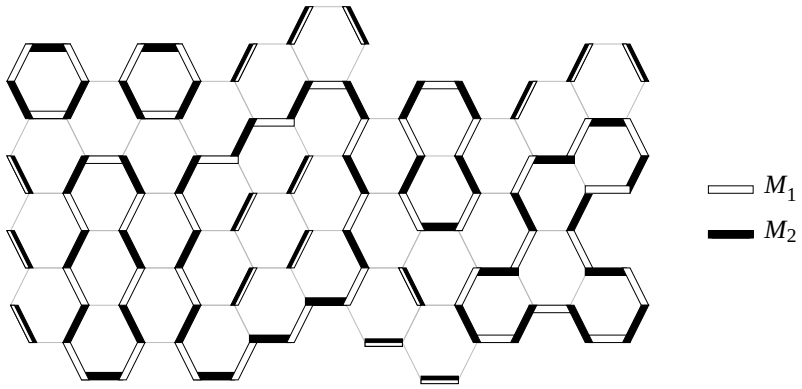

Figure 2.4: Superimposition of two dimer configurations M_1 and M_2 of a subgraph G of the honeycomb lattice $\mathbb{H}$.

One can transform the matching M_1 into the matching M_2, by replacing edges of M_1 by those of M_2 in all alternating cycles of length ≥ 4 of the superimposition. Thus, arguing by induction, it suffices to show that the sign of the contributions of M_1 and M_2 to $\det(K)$ is the same when M_1 and M_2 differ along a single alternating cycle of length ≥ 4. Let us assume that this is the case, denote the unique cycle by C and by $\mathsf{w}_{i_1}, \mathsf{b}_{j_1}, \dots, \mathsf{w}_{i_k}, \mathsf{b}_{j_k}$ its vertices in clockwise order, see Figure 2.5.

Let σ (resp. τ) be the permutation corresponding to M_1 (resp. M_2). Then by the correspondence between enumeration of matchings and terms in the expansion of the determinant, we have:

$$j_1 = \sigma(i_1) = \tau(i_2),\ j_2 = \sigma(i_2) = \tau(i_3),\ \dots,\ j_k = \sigma(i_k) = \tau(i_1).$$

If we let c be the permutation cycle $c = (i_k \dots i_1)$, then we deduce:

$$\tau(i_\ell) = \sigma(i_{\ell-1}) = \sigma \circ c(i_\ell). \tag{2.1}$$

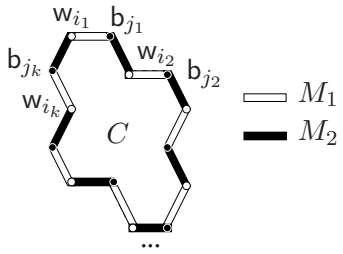

Figure 2.5: Labeling of the vertices of an example of superimposition cycle of M_1 and M_2.

In order to check that the contributions of M_1 and M_2 to $\det(K)$ have the same sign, it suffices to check that the sign of the ratio of the contributions is positive. The sign of this ratio, denoted by $\mathrm{Sign}(M_1/M_2)$, is:

$$\mathrm{Sign}(M_1/M_2) = \mathrm{Sign}\left(\frac{\mathrm{sgn}(\sigma)}{\mathrm{sgn}(\tau)}\frac{K(\mathsf{w}_{i_1},\mathsf{b}_{\sigma(i_1)})\dots K(\mathsf{w}_{i_k},\mathsf{b}_{\sigma(i_k)})}{K(\mathsf{w}_{i_1},\mathsf{b}_{\tau(i_1)})\dots K(\mathsf{w}_{i_k},\mathsf{b}_{\tau(i_k)})}\right),$$

which is the same as the sign of the product of the numerator and the denominator. Now,

$$\begin{aligned}
(\diamond_1) :&= \mathrm{sgn}(\sigma)\mathrm{sgn}(\tau) = \mathrm{sgn}(\sigma\circ\tau) = \mathrm{sgn}(\sigma\circ\sigma\circ c) \quad \text{by Equation (2.1)}\\
&= (-1)^{k+1}.\\
(\diamond_2) :&= \mathrm{Sign}\big(\,[K(\mathsf{w}_{i_1},\mathsf{b}_{\sigma(i_1)})\dots K(\mathsf{w}_{i_k},\mathsf{b}_{\sigma(i_k)})][K(\mathsf{w}_{i_1},\mathsf{b}_{\tau(i_1)})\dots K(\mathsf{w}_{i_k},\mathsf{b}_{\tau(i_k)})]\big)\\
&= \mathrm{Sign}\big([K(\mathsf{w}_{i_1},\mathsf{b}_{j_1})\dots K(\mathsf{w}_{i_k},\mathsf{b}_{j_k})][K(\mathsf{w}_{i_1},\mathsf{b}_{j_k})\dots K(\mathsf{w}_{i_k},\mathsf{b}_{j_{k-1}})]\big)\\
&= \mathrm{Sign}\big(K(\mathsf{w}_{i_1},\mathsf{b}_{j_1})K(\mathsf{w}_{i_1},\mathsf{b}_{j_k})\dots K(\mathsf{w}_{i_k},\mathsf{b}_{j_k})K(\mathsf{w}_{i_k},\mathsf{b}_{j_{k-1}})\big)
\end{aligned}$$

Let p be the parity of the number of edges of the cycle C oriented clockwise. The cycle C is said to be *clockwise odd* if $p=1$, *clockwise even* if $p=0$. Let us show that $\mathrm{Sign}(M_1/M_2)=+1$ if and only if $p=1$. To this purpose, we first relate $(\diamond_2)$ and $(-1)^p$.

Partition $\mathsf{W}_C := \{\mathsf{w}_{i_1},\dots,\mathsf{w}_{i_k}\}$ as $\mathsf{W}_C^e \cup \mathsf{W}_C^o$, where W_C^e consists of white vertices with 0 or 2 incoming edges (equivalently 2 or 0 outgoing edges), and W_C^o consists of white vertices with one incoming and one outgoing edge, then $|\mathsf{W}_C^e| + |\mathsf{W}_C^o| = k$. If a white vertex belongs to W_C^e, it contributes 1 to $(\diamond_2)$ and 1 to p; if a white vertex belongs to W_C^o, it contributes -1 to $(\diamond_2)$ and 0 to p. We thus have:

$$\begin{cases}(\diamond_2) & = (-1)^{|\mathsf{W}_C^o|}\\ (-1)^p & = (-1)^{|\mathsf{W}_C^e|}\end{cases} \Rightarrow\ (\diamond_2) = (-1)^k(-1)^p.$$

As a consequence $\mathrm{Sign}(M_1/M_2) = (\diamond_1)(\diamond_2) = (-1)^{2k+1}(-1)^p$, so that $\mathrm{Sign}(M_1/M_2)$ is positive if and only if $p=1$, *i.e.* if and only if the cycle C is clockwise odd.

Following Kasteleyn [Kas67], an orientation of the edges of G such that all cycles obtained as superimposition of dimer configurations are clockwise odd, is called *admissible*. Define a *contour cycle* to be a cycle bounding an inner face of the graph G. Kasteleyn proves that if the orientation is such that all contour cycles are clockwise odd, then the orientation is admissible. The proof is by induction on the number of faces included in the cycle, refer to the paper [Kas67] for details. An orientation of the edges of G such that all contour cycles are clockwise odd is constructed in the following way, see for example [CR07]. Consider a spanning tree of the dual graph G^*, with a vertex corresponding to the outer face, taken to be the root of the tree. Choose any orientation for edges of G not crossed by the spanning tree. Then, start from a leaf of the tree, and orient

the dual of the edge connecting the leaf to the tree in such a way that the contour cycle of the corresponding face is clockwise odd. Remove the leaf and the edge from the tree. Iterate until only the root remains. Since the tree is spanning, all faces are reached by the algorithm, and by construction all corresponding contour cycles are clockwise odd.

A *Kasteleyn-Percus matrix*, or simply *Kasteleyn matrix*, denoted by K, associated to the graph G is the oriented, weighted adjacency matrix corresponding to an admissible orientation. We have thus proved the following:

Theorem 1. [Kas67] *Let G be a finite, planar bipartite graph with an admissible orientation of its edges, let ν be a positive weight function on the edges, and K be the corresponding Kasteleyn matrix. Then, the partition function of the graph G is:*

$$Z(\mathsf{G}) = |\det(K)|.$$

When the graph G is not bipartite, lines and columns of the adjacency matrix are indexed by all vertices of G (vertices cannot be naturally split into two subsets). By choosing an admissible orientation of the edges, the partition function can be expressed as the square root of the determinant of the corresponding Kasteleyn matrix or, since this matrix is skew-symmetric, as the Pfaffian of this same matrix. For more details, refer to [Kas67].

2.3.2 Boltzmann measure formula

When the graph G is bipartite, Kenyon [Ken97] gives an explicit expression for the local statistics of the Boltzmann measure. Let K be a Kasteleyn matrix associated to G, and let $\{\mathsf{e}_1 = \mathsf{w}_1\mathsf{b}_1, \ldots, \mathsf{e}_k = \mathsf{w}_k\mathsf{b}_k\}$ be a subset of edges of G.

Theorem 2. [Ken97] *The probability $\mu(\mathsf{e}_1, \ldots, \mathsf{e}_k)$ of edges $\{\mathsf{e}_1, \ldots, \mathsf{e}_k\}$ occurring in a dimer configuration of G chosen with respect to the Boltzmann measure μ is:*

$$\mu(\mathsf{e}_1, \ldots, \mathsf{e}_k) = \left| \left(\prod_{i=1}^{k} K(\mathsf{w}_i, \mathsf{b}_i) \right) \det_{1 \leq i,j \leq k} K^{-1}(\mathsf{b}_i, \mathsf{w}_j) \right|. \tag{2.2}$$

Proof. The weighted sum of dimer configurations containing the edges $\{\mathsf{e}_1, \ldots, \mathsf{e}_k\}$ is (up to sign) the sum of all terms containing $K(\mathsf{w}_1, \mathsf{b}_1) \ldots K(\mathsf{w}_k, \mathsf{b}_k)$ in the expansion of $\det(K)$. By expanding this determinant along lines (or columns), it is easy to see by induction that this is equal to:

$$\left| \left(\prod_{i=1}^{k} K(\mathsf{w}_i, \mathsf{b}_i) \right) \det(K_E) \right|,$$

where K_E is the matrix obtained from K by removing the lines corresponding to $\mathsf{w}_1, \ldots, \mathsf{w}_k$ and the columns corresponding to $\mathsf{b}_1, \ldots, \mathsf{b}_k$. Now by Jacobi's identity, see for example [HJ90]:

$$\det(K_E) = \det(K) \det\left((K^{-1})_{E^*}\right),$$

where E^* is the set of edges not in E. Otherwise stated, $(K^{-1})_{E^*}$ is the $k \times k$ matrix obtained from K^{-1} by keeping the lines corresponding to $\mathsf{b}_1, \ldots, \mathsf{b}_k$ and the columns corresponding to $\mathsf{w}_1, \ldots, \mathsf{w}_k$. Thus,

$$\mu(\mathsf{e}_1, \ldots, \mathsf{e}_k) = \frac{\left| \left(\prod_{i=1}^{k} K(\mathsf{w}_i, \mathsf{b}_i) \right) \det(K_E) \right|}{|\det(K)|} = \left| \left(\prod_{i=1}^{k} K(\mathsf{w}_i, \mathsf{b}_i) \right) \det\left((K^{-1})_{E^*}\right) \right|.$$

□

Remark 3. Edges form a *determinantal point process* with respect to the counting measure, that is a point process such that the joint probabilities are of the form

$$\mu(\mathsf{e}_1, \ldots, \mathsf{e}_k) = \det(M(\mathsf{e}_i, \mathsf{e}_j)_{1 \leq i,j \leq k}),$$

for some kernel M. In the case of bipartite dimers, $M(\mathsf{e}_i, \mathsf{e}_j) = K(\mathsf{w}_i, \mathsf{b}_j)K^{-1}(\mathsf{b}_i, \mathsf{w}_j)$, see [Sos07] for an overview.

2.3.3 Explicit example

Figure 2.6 gives an example of a planar, bipartite graph whose edges are assigned positive weights and an admissible orientation.

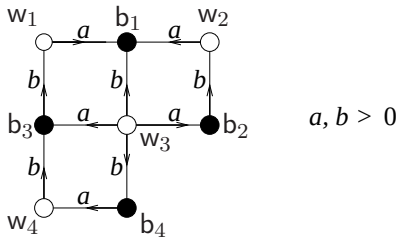

Figure 2.6: A planar, bipartite graph with a positive weight function and an admissible orientation.

The corresponding Kasteleyn matrix is:

$$K = \begin{pmatrix} a & 0 & -b & 0 \\ a & -b & 0 & 0 \\ b & a & a & b \\ 0 & 0 & b & -a \end{pmatrix},$$

and the determinant is equal to

$$\det(K) = 2a^3b + 2b^3a.$$

Setting $a = b = 1$ yields that the number of perfect matchings of this graph is 4. In this case, the Boltzmann measure is the uniform measure on tilings of this graph.

The inverse Kasteleyn matrix K^{-1} is:

$$K^{-1} = \frac{1}{4}\begin{pmatrix} 2 & 1 & 1 & 1 \\ 2 & -3 & 1 & 1 \\ -2 & 1 & 1 & 1 \\ -2 & 1 & 1 & -3 \end{pmatrix}.$$

Using the labeling of the vertices of Figure 2.6 and Theorem 2, we compute the probability of occurrence of some subset of edges:

$$\mu(\mathsf{w}_1\mathsf{b}_1) = |K^{-1}(\mathsf{b}_1, \mathsf{w}_1)| = \frac{1}{2}$$

$$\mu(\mathsf{w}_3\mathsf{b}_1) = |K^{-1}(\mathsf{b}_1, \mathsf{w}_3)| = \frac{1}{4}$$

$$\mu(\mathsf{w}_1\mathsf{b}_1, \mathsf{w}_3\mathsf{b}_4) = \left|\det \begin{pmatrix} K^{-1}(\mathsf{b}_1, \mathsf{w}_1) & K^{-1}(\mathsf{b}_1, \mathsf{w}_3) \\ K^{-1}(\mathsf{b}_4, \mathsf{w}_1) & K^{-1}(\mathsf{b}_4, \mathsf{w}_3) \end{pmatrix}\right| = \frac{1}{16}\left|\det \begin{pmatrix} 2 & 1 \\ -2 & 1 \end{pmatrix}\right| = \frac{1}{4}.$$

You can try and compute other probabilities. In this simple case, it is actually easier to explicitly find all possible configurations (4 of them), and compute the probabilities. However, the goal of this example is to show how to use the general formulae.

2.4 Geometric interpretation of lozenge tilings

By means of the height function, Thurston interprets lozenge tilings of the triangular lattice as discrete surfaces in a rotated version of $\mathbb{Z}^3$ projected onto the plane. He gives a similar interpretation of domino tilings of the square lattice. This approach can be generalized to dimer configurations of bipartite graphs using flows. This yields an interpretation of the dimer model on a bipartite graph as a random interface model in dimensions $2+1$, and offers more insight into the model. In this section we exhibit Thurston's construction of the height function on lozenge tilings. We postpone the definition of the height function on general bipartite graphs until Section 3.1.

Faces of the triangular lattice $\mathbb{T}$ can be colored in black and white, so that black faces (resp. white ones) are only adjacent to white ones (resp. black ones). This is a consequence of the fact that its dual graph, the honeycomb lattice, is bipartite. Orient the black faces counterclockwise, and the white ones clockwise, see Figure 2.7 (left). Consider a finite subgraph X of $\mathbb{T}$ which is tileable by lozenges, and a lozenge tiling T of X. Then the height function h^T is an integer valued function on vertices of X, defined inductively as follows:

- Fix a vertex v_0 of X, and set $h^T(\mathsf{v}_0) = 0$.
- For every boundary edge uv of a lozenge, $h^T(\mathsf{v}) - h^T(\mathsf{u}) = +1$ if the edge uv is oriented from u to v, implying that $h^T(\mathsf{v}) - h^T(\mathsf{u}) = -1$ when the edge uv is oriented from v to u.

The height function is well defined, in the sense that the height change around any oriented cycle is 0. An example of computation of the height function is given in Figure 2.7 (right).

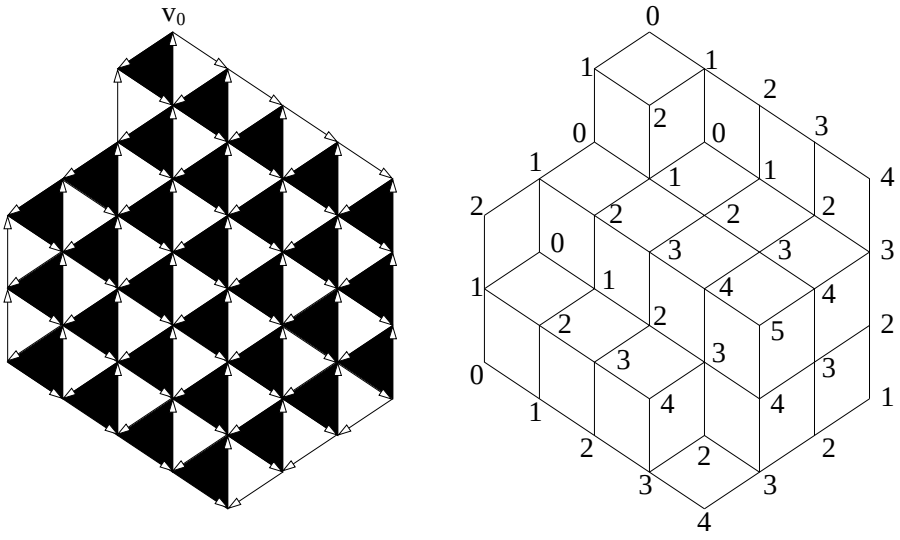

Figure 2.7: Orientation of faces of the triangular lattice (left). Height function corresponding to a lozenge tiling (right).

As a consequence, lozenge tilings are interpreted as stepped surfaces in $\widetilde{\mathbb{Z}^3}$ projected onto the plane, where $\widetilde{\mathbb{Z}^3}$ is $\mathbb{Z}^3$ rotated so that diagonals of the cubes are orthogonal to the plane. The height function is then simply the "height" of the surface (*i.e.* third coordinate). This construction gives a mathematical sense to the intuitive feeling of cubes sticking in or out, which strikes us when watching a picture of lozenge tilings.

Height functions characterize lozenge tilings as stated by the following lemma.

Lemma 4. *Let* X *be a finite simply connected subgraph of the triangular lattice* $\mathbb{T}$*, which is tileable by lozenges. Let* h *be an integer valued function on the vertices of* X*, satisfying:*

- $h(\mathsf{v}_0) = 0$*, where* v_0 *is a fixed vertex of* X*.*
- $h(\mathsf{v}) - h(\mathsf{u}) = 1$ *for any boundary edge* uv *of* X *oriented from* u *to* v*.*
- $h(\mathsf{v}) - h(\mathsf{u}) = 1$ *or* -2 *for any interior edge* uv *of* X *oriented from* u *to* v*.*

Then, there is a bijection between functions h *satisfying these two conditions, and tilings of* X*.*

Proof. Let T be a lozenge tiling of X and let uv be an edge of X, oriented from u to v. Then, the edge uv is either a boundary edge or a diagonal of a lozenge. By definition of the height function, the height change is 1 in the first case, and -2 in the second.

Conversely, let h be an integer function as in the lemma. Let us construct a tiling T whose height function is h. Consider a black face of X, then there is exactly one edge uv on the boundary of this face whose height change is -2. To this face, we associate the lozenge which is crossed by the edge uv. Repeating this procedure for all black faces yields a tiling of X. □

Thurston [Thu90] uses height functions in order to determine whether a subgraph of the triangular lattice can be tiled by lozenges. Refer to the paper for details.

Chapter 3

Dimer model on infinite periodic bipartite graphs

This chapter is devoted to the paper "Dimers and amoebas" [KOS06] by Kenyon, Okounkov and Sheffield.

Recall that edges of dimer configurations represent di-atomic molecules. Since we are interested in the macroscopic behavior of the system, our goal is to study the model on very large graphs. It turns out that it is easier to extract information for the model defined on infinite graphs, rather than very large ones. Indeed, on very large but finite graphs, Kasteleyn's computation can be done, but involves computing the determinant of huge matrices, which is of course very hard in general, and won't tell us much about the system. Computing explicitly the local statistics of the Boltzmann measure becomes hardly tractable since it requires inverting very large matrices. This motivates the following road map.

- Assume that the graph $\mathsf{G} = (\mathsf{V}, \mathsf{E})$ is simple, planar, infinite, bipartite, and $\mathbb{Z}^2$-periodic. This means that G is embedded in the plane so that translations act by color-preserving isomorphism of G, *i.e.* isomorphisms which map black vertices to black ones and white vertices to white ones. For later purposes, we consider the underlying lattice $\mathbb{Z}^2$ to be a subgraph of the dual graph G^*, and fix a basis $\{e_x, e_y\}$, allowing to record copies of a vertex v of G as $\{\mathsf{v} + (k,l) : (k,l) \in \mathbb{Z}^2\}$. Refer to Figure 3.1 for an example when G is the square-octagon graph.

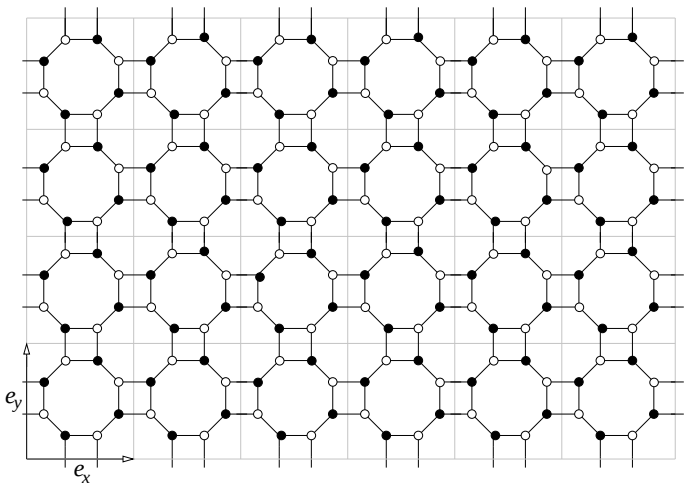

Figure 3.1: A piece of the square-octagon graph. The underlying lattice $\mathbb{Z}^2$ is in light grey, the two black vectors represent a choice of basis $\{e_x, e_y\}$.

- Let $\mathsf{G}_n = (\mathsf{V}_n, \mathsf{E}_n)$ be the quotient of G by the action of $n\mathbb{Z}^2$. Then the sequence of graphs $\{\mathsf{G}_n\}_{n\geq 1}$ is an exhaustion of the infinite graph G by toroidal graphs. The graph $\mathsf{G}_1 = \mathsf{G}/\mathbb{Z}^2$ is called the *fundamental domain*, see Figure 3.2. Assume that edges of G_1 are assigned a positive weight function ν thus defining a periodic weight function on the edges of G.

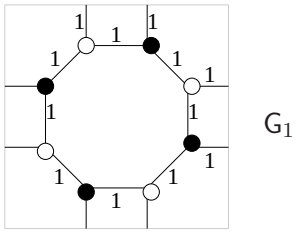

Figure 3.2: Fundamental domain G_1 of the square-octagon graph, opposite sides in light grey are identified. Edges are assigned weight 1.

- The goal of this chapter is to understand the dimer model on G, using the exhaustion $\{\mathsf{G}_n\}_{n\geq 1}$, by taking limits as $n \to \infty$ of appropriate quantities.

Note that it is crucial to take an exhaustion of G by toroidal graphs. Indeed, the latter are invariant by translations in two directions, a key fact which allows computations to go through using Fourier techniques. Note also that taking an exhaustion by planar graphs a priori leads to different results because of the influence of the boundary which cannot be neglected.

Although it might not seem so clear at this stage, the fact that G and $\{\mathsf{G}_n\}_{n\geq 1}$ are assumed to be bipartite is also crucial for the results of this chapter, because it allows to relate the dimer model to well behaved algebraic curves. Having a general theory of the dimer model on non-bipartite graphs is one of the important open questions of the field.

3.1 Height function

In this section, we describe the construction of the *height function* on dimer configurations of the infinite graph G and of the toroidal graphs G_n, $n \geq 1$. Since we are working on the dimer model and not on the tiling model, as in Thurston's construction, the height function is a function on faces of G or equivalently, a function on vertices of the dual graph G^*.

The definition of the height function relies on *flows*. Denote by $\vec{\mathsf{E}}$ the set of directed edges of the graph G, *i.e.* every edge of E yields two oriented edges of $\vec{\mathsf{E}}$. A *flow* ω is a real valued function defined on $\vec{\mathsf{E}}$, that is every directed edge (u,v) of $\vec{\mathsf{E}}$ is assigned a flow $\omega(\mathsf{u},\mathsf{v})$.

The *divergence* of a flow ω, denoted by $\operatorname{div}\omega$, is a real valued function defined on V giving the difference between total outflow and total inflow at vertices:

$$\forall\, u \in \mathsf{V}, \quad \operatorname{div}\omega(\mathsf{u}) = \sum_{\mathsf{v}\sim\mathsf{u}} \omega(\mathsf{u},\mathsf{v}) - \sum_{\mathsf{v}\sim\mathsf{u}} \omega(\mathsf{v},\mathsf{u}).$$

Since G is bipartite, we split vertices V into white and black ones: $\mathsf{V} = \mathsf{W} \cup \mathsf{B}$. Then, every dimer configuration M of G defines a white-to-black unit flow ω^M as follows. The flow ω^M takes value 0 on all directed edges arising from edges of E which do not belong to M, and

$$\forall\, \mathsf{wb} \in M, \quad \omega^M(\mathsf{w},\mathsf{b}) = 1, \quad \omega^M(\mathsf{b},\mathsf{w}) = 0.$$

Since every vertex of the graph G is incident to exactly one edge of the perfect matching M, the flow ω^M has divergence 1 at every white vertex, and -1 at every black one, that is:

$$\forall\, \mathsf{w} \in \mathsf{W},\ \operatorname{div}\omega^M(\mathsf{w}) = \sum_{\mathsf{b}\sim\mathsf{w}} \omega^M(\mathsf{w},\mathsf{b}) - \sum_{\mathsf{b}\sim\mathsf{w}} \omega^M(\mathsf{b},\mathsf{w}) = 1,$$
$$\forall\, \mathsf{b} \in \mathsf{B},\ \operatorname{div}\omega^M(\mathsf{b}) = \sum_{\mathsf{w}\sim\mathsf{b}} \omega^M(\mathsf{b},\mathsf{w}) - \sum_{\mathsf{w}\sim\mathsf{b}} \omega^M(\mathsf{w},\mathsf{b}) = -1.$$

Let M_0 be a fixed periodic reference perfect matching of G, and ω^{M_0} be the corresponding flow, called the *reference flow*. Then, for any other matching M with flow ω^M, the difference $\omega^M - \omega^{M_0}$ is a divergence-free flow, that is:

$$\begin{aligned}\forall\, \mathsf{w} \in \mathsf{W},\ \operatorname{div}(\omega^M - \omega^{M_0})(\mathsf{w}) &= \sum_{\mathsf{b}\sim\mathsf{w}} (\omega^M(\mathsf{w},\mathsf{b}) - \omega^{M_0}(\mathsf{w},\mathsf{b})) - \sum_{\mathsf{b}\sim\mathsf{w}} (\omega^M(\mathsf{b},\mathsf{w}) - \omega^{M_0}(\mathsf{b},\mathsf{w})) \\ &= \operatorname{div}\omega^M(\mathsf{w}) - \operatorname{div}\omega^{M_0}(\mathsf{w}) = 1 - 1 = 0,\end{aligned}$$

and similarly for black vertices.

We are now ready to define the height function. Let M be a dimer configuration of G, then the *height function* h^M is an integer valued function on faces of G defined as follows.

- Fix a face f_0 of G, and set $h^M(\mathsf{f}_0) = 0$.
- For any other face f_1, consider an edge-path γ of the dual graph G^*, from f_0 to f_1. Let $(\mathsf{u}_1,\mathsf{v}_1),\dots,(\mathsf{u}_k,\mathsf{v}_k)$ denote edges of G crossing the path γ, where for every i, u_i is on the left of the path γ and v_i on the right. Then $h^M(\mathsf{f}_1) - h^M(\mathsf{f}_0)$ is the *total flux* of $\omega^M - \omega^{M_0}$ across γ, that is:

$$h^M(\mathsf{f}_1) - h^M(\mathsf{f}_0) = \sum_{i=1}^{k} [(\omega^M(\mathsf{u}_i,\mathsf{v}_i) - \omega^M(\mathsf{v}_i,\mathsf{u}_i)) - (\omega^{M_0}(\mathsf{u}_i,\mathsf{v}_i) - \omega^{M_0}(\mathsf{v}_i,\mathsf{u}_i))].$$

The height function is well defined if it is independent of the choice of γ, or equivalently if the height change around every face f^* of the dual graph G^* is 0. Let u be the vertex of the graph G corresponding to the face f^*, and let $\mathsf{v}_1,\dots,\mathsf{v}_k$ be its neighbors. Then, by definition, the height change around the face f^*, in counterclockwise order, is:

$$\sum_{i=1}^{k} [(\omega^M(\mathsf{u},\mathsf{v}_i) - \omega^M(\mathsf{v}_i,\mathsf{u})) - (\omega^{M_0}(\mathsf{u},\mathsf{v}_i) - \omega^{M_0}(\mathsf{v}_i,\mathsf{u}))] = \operatorname{div}(\omega^M - \omega^{M_0})(\mathsf{u}) = 0.$$

The height function is thus well defined as a consequence of the fact that the flow $\omega^M - \omega^{M_0}$ is divergence free, up to the choice of a base face f_0 and of a reference matching M_0. An analog of Lemma 4 gives a bijection between height functions and dimer configurations of G.

Remark 5.

- There is actually an easy way of computing the height function. Recall from Section 2.3 that the superimposition of two dimer configurations M and M_0 consists of doubled edges and alternating cycles of length ≥ 4 (cycles may extend to infinity when G is infinite). Let us denote by $M - M_0$ the oriented superimposition of M and M_0, with edges of M oriented from white vertices to black ones, and those of M_0 from black vertices to white ones, then $M - M_0$ consists of doubled edges oriented in both directions and oriented alternating cycles of length ≥ 4, see for example Figure 3.3. Returning to the definition of the height function, one notices that the height changes by ± 1 exactly when crossing a cycle, and the sign only depends on the orientation of the cycle.

- By taking a different choice of reference flow, one can recover Thurston's height function in the case of lozenge and domino tilings, up to a global multiplicative factor of $\frac{1}{3}$ in the first case, and $\frac{1}{4}$ in the second - the interested reader can try and work out this relation explicitly.

Let us now consider the toroidal graph $\mathsf{G}_n = \mathsf{G}/n\mathbb{Z}^2$. In this case, the height function is not well defined since there might be some period, or height change, along cycles in the dual graph winding around the torus horizontally or vertically, see Figure 3.3. More precisely, a perfect matching M of G_n can be lifted to a perfect matching of the infinite graph G, also denoted M. Then, the perfect matching M of G_n is said to have *height change* (h_x^M, h_y^M) if:

$$h^M(\mathsf{f} + (n, 0)) = h^M(\mathsf{f}) + h_x^M$$
$$h^M(\mathsf{f} + (0, n)) = h^M(\mathsf{f}) + h_y^M.$$

Note that height change is well defined, *i.e.* does not depend on the choice of face f, because the flow $\omega^M - \omega^{M_0}$ is divergence-free.

Figure 3.3 gives an example of the reference perfect matching M_0 induced by a periodic reference matching of G, and of the height change computation of a dimer configuration M of the toroidal graph G_2 of the square-octagon graph. The perfect matching M has height change $(0, 1)$.

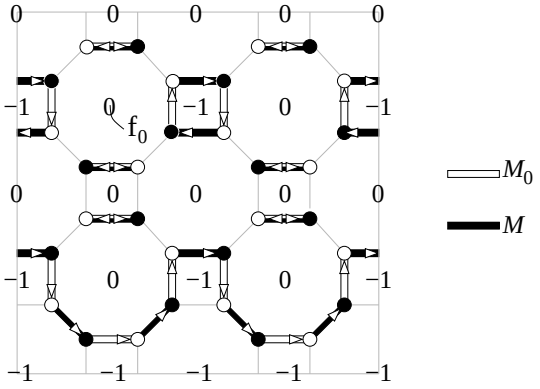

Figure 3.3: A perfect matching M of the toroidal graph G_2, having height change $(0, 1)$.

Remark 6. Let $\mathbb{T}^2 = \{(z, w) \in \mathbb{C}^2 : |z| = |w| = 1\}$ denote the two-dimensional unit torus, and let $H_1(\mathbb{T}^2, \mathbb{Z}) \cong \mathbb{Z}^2$ be the first homology group of $\mathbb{T}^2$ in $\mathbb{Z}$. The graph G_n being embedded in $\mathbb{T}^2$, we take as representative of a basis of $H_1(\mathbb{T}^2, \mathbb{Z})$ the vectors ne_x and ne_y embedded on the torus, where recall $\{e_x, e_y\}$ were our choice of basis vector for $\mathbb{Z}^2$, see Figure 3.1. In the case of the square-octagon graph and G_2 of Figure 3.3, the first basis vector is the light grey horizontal cycle oriented from left to right, and the second is the light grey vertical cycle oriented from bottom to top. Then, the homology class of the oriented superimposition $M - M_0$ in this basis is $(1, 0)$, and the height change is $(0, 1)$. More generally, if the homology class of $M - M_0$ is (a, b), then the height change (h_x^M, h_y^M) is $(-b, a)$. This is because, as mentioned in Remark 5, the height function changes by ± 1 exactly when it crosses oriented cycles of $M - M_0$, implying that the height change (h_x^M, h_y^M) can be identified through the intersection pairing with the homology class of the oriented configuration $M - M_0$ in $H_1(\mathbb{T}^2, \mathbb{Z})$.

3.2 Partition function, characteristic polynomial, free energy

Let us recall the setting: G is a simple, planar, infinite, bipartite $\mathbb{Z}^2$-periodic graph, and $\{\mathsf{G}_n\}_{n\geq 1}$ is the corresponding toroidal exhaustion. Edges of G are assigned a periodic, positive weight function ν, and $\{e_x, e_y\}$ denotes a choice of basis of the underlying lattice $\mathbb{Z}^2$.

In this section we present the computation of the partition function for dimer configurations of the toroidal graph G_n, and the computation of the free energy, which is minus the exponential growth rate of the partition function of the exhaustion G_n. More precisely, Section 3.2.1 is devoted to Kasteleyn theory on the torus. Then, in Section 3.2.2 we define the *characteristic polynomial*, one of the key objects underlying the dimer model on bipartite graphs, yielding a compact closed formula for the partition function, see Corollary 10. With this expression at hand, one then derives the explicit formula for the free energy, see Theorem 11.

3.2.1 Kasteleyn matrix

In Section 2.3, we proved that the partition function of a finite, simply connected planar graph is given by the determinant of a Kasteleyn matrix. When the graph is embedded on the torus, a single determinant is not enough, what is needed is a linear combination of determinants determined in the following way.

Consider the fundamental domain G_1 and let K_1 be a Kasteleyn matrix of this graph, that is K_1 is the oriented, weighted, adjacency matrix of G_1 for a choice of admissible orientation of the edges. Note that admissible orientations also exist for graphs embedded in the torus. Let us now look at the signs of the weighted matchings in the expansion of $\det(K_1)$. Consider a fixed reference matching M_0 of G_1, and let M be any other matching of G_1. Then, by the results of [Kas67, DZM+96, GL99, Tes00, CR07], the sign of the matching M only depends on the parity of the vertical and horizontal height change. Moreover, of the four possible parity classes, three have the same sign in $\det(K_1)$ and one has opposite sign. By an appropriate choice of admissible orientation, one can make the $(0,0)$ class have positive sign.

Let γ_x, γ_y be the basis vector e_x, e_y of the underlying lattice $\mathbb{Z}^2$, embedded on the torus. Since we have chosen $\mathbb{Z}^2$ to be a subgraph of the dual graph G^*, γ_x, γ_y are oriented cycles of the dual graph G_1^*, see Figure 3.4. We refer to γ_x as a horizontal cycle, and to γ_y as a vertical one.

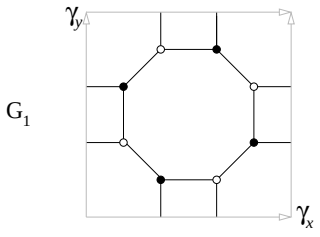

Figure 3.4: Fundamental domain G_1 of the square octagon graph with the oriented paths γ_x, γ_y in the dual graph G_1^*. The two copies of γ_x, respectively γ_y, are glued together.

For $\sigma, \tau \in \{0,1\}$, let $K_1^{\theta\tau}$ be the Kasteleyn matrix in which the weights of the edges crossing the horizontal cycle γ_x are multiplied by $(-1)^\theta$, and those crossing the vertical cycle γ_y are multiplied by $(-1)^\tau$. Observing that changing the signs along a horizontal dual cycle has the effect of negating the weight of matchings with odd horizontal height change, and similarly for

vertical; the following table indicates the sign of the matchings in the expansion of $\det(K_1^{\theta\tau})$, as a function of the horizontal and vertical height change mod 2.

	$(0,0)$	$(1,0)$	$(0,1)$	$(1,1)$
$\det(K_1^{00})$	$+$	$-$	$-$	$-$
$\det(K_1^{10})$	$+$	$+$	$-$	$+$
$\det(K_1^{01})$	$+$	$-$	$+$	$+$
$\det(K_1^{11})$	$+$	$+$	$+$	$-$

(3.1)

From Table 3.1, we deduce

$$Z(\mathsf{G}_1) = \frac{1}{2}\left(-\det(K_1^{00}) + \det(K_1^{10}) + \det(K_1^{01}) + \det(K_1^{11})\right). \tag{3.2}$$

A similar argument holds for the toroidal graph G_n, $n \geq 1$. The orientation of edges of G_1 defines a periodic orientation of edges of G, and thus an orientation of edges of G_n. Let $\gamma_{x,n}$, $\gamma_{y,n}$ be the oriented cycles in the dual graph G_n^*, obtained by taking n times the basis vector e_x, n times the basis vector e_y respectively, embedded on the torus. For $\sigma, \tau \in \{0,1\}$, let $K_n^{\sigma\tau}$ be the matrix K_n in which the weights of edges crossing the horizontal cycle $\gamma_{x,n}$ are multiplied by $(-1)^\theta$, and those crossing the vertical cycle $\gamma_{y,n}$ are multiplied by $(-1)^\tau$. Then,

Theorem 7. [Kas67, DZM+96, GL99, Tes00, CR07, CR08]

$$Z(\mathsf{G}_n) = \frac{1}{2}\left(-\det(K_n^{00}) + \det(K_n^{10}) + \det(K_n^{01}) + \det(K_n^{11})\right).$$

3.2.2 Characteristic polynomial

Let K_1 be a Kasteleyn matrix of the fundamental domain G_1. Given complex numbers z and w, an altered Kasteleyn matrix $K_1(z,w)$ is constructed as follows. Let γ_x, γ_y be the oriented horizontal and vertical cycles of G_1^*. Then, multiply edge-weights of edges crossing γ_x by z whenever the white vertex is on the left, and by z^{-1} whenever the black vertex is on the left. Similarly, multiply edge-weights of edges crossing the vertical path γ_y by $w^{\pm 1}$, see Figure 3.5.

The *characteristic polynomial* $P(z,w)$ of the graph G_1 is defined as the determinant of the altered Kasteleyn matrix:

$$P(z,w) = \det(K_1(z,w)).$$

As we will see, the characteristic polynomial contains most of the information on the macroscopic behavior of the dimer model on the graph G.

The next very useful lemma expresses the characteristic polynomial using height changes of dimer configurations of G_1. Refer to Section 3.1 for definitions and notations concerning height changes. Let M_0 be a reference dimer configuration of G_1, and suppose the admissible orientation of the edges is chosen such that perfect matchings having $(0,0)$ mod $(2,2)$ height change have $+$ sign in the expansion of $\det(K_1)$. We consider the altered Kasteleyn matrix $K_1(z,w)$ constructed from K_1. Let ω^{M_0} be the reference flow corresponding to the reference dimer configuration M_0, and let x_0 denote the total flux of ω^{M_0} across γ_x, similarly y_0 is the total flux of ω^{M_0} across γ_y. Then, we have:

Lemma 8. [KOS06]

$$P(z,w) = z^{x_0} w^{y_0} \sum_{M \in \mathcal{M}(\mathsf{G}_1)} \nu(M) z^{h_x^M} w^{h_y^M} (-1)^{h_x^M h_y^M + h_x^M + h_y^M}, \tag{3.3}$$

where, for every dimer configuration M of $\mathcal{M}(\mathsf{G}_1)$, (h_x^M, h_y^M) is the height change of M.

Proof. Let M be a perfect matching of G_1. Then, by the choice of Kasteleyn orientation, the sign of the term corresponding to M in the expansion of $\det(K_1(z,w))$ is: $+$ if $(h_x^M, h_y^M) = (0,0) \bmod (2,2)$, and $-$ else. This can be summarized as:

$$(-1)^{h_x^M h_y^M + h_x^M + h_y^M}.$$

Let us denote by $\nu_{z,w}$, the weight function on edges of G_1 obtained from G_1 by multiplying edge-weights of edges crossing γ_x by $z^{\pm 1}$, and those crossing γ_y by $w^{\pm 1}$ as above. Then,

$$\nu_{z,w}(M) = \nu(M) z^{n_x^{\mathsf{wb}}(M) - n_x^{\mathsf{bw}}(M)} w^{n_y^{\mathsf{wb}}(M) - n_y^{\mathsf{bw}}(M)},$$

where $n_x^{\mathsf{wb}}(M)$ is the number of edges of M crossing γ_x, which have a white vertex on the left of γ_x, and $n_x^{\mathsf{bw}}(M)$ is the number of edges of M crossing γ_x, which have a black vertex on the left of γ_x. The definition of $n_y^{\mathsf{wb}}(M)$, $n_y^{\mathsf{bw}}(M)$ is similar with γ_x replaced by γ_y.

Returning to the definition of the height change for dimer configurations of the toroidal graph G_n, we have:

$$h_x^M = n_x^{\mathsf{wb}}(M) - n_x^{\mathsf{bw}}(M) - n_x^{\mathsf{wb}}(M_0) + n_x^{\mathsf{bw}}(M_0),$$

so that:

$$n_x^{\mathsf{wb}}(M) - n_x^{\mathsf{bw}}(M) = h_x^M + n_x^{\mathsf{wb}}(M_0) - n_x^{\mathsf{bw}}(M_0) = h_x^M + x_0,$$

since by definition x_0 is the total flux of ω^{M_0} across γ_x. Computing h_y^M in a similar way yields the lemma. □

Example 3.1. Let us compute the characteristic polynomial of the fundamental domain G_1 of the square-octagon graph, with weights one on the edges. Figure 3.5 (left) describes the labeling of the vertices, and weights of the altered Kasteleyn matrix. The orientation of the edges is admissible and is such that perfect matchings having $(0,0)$ height change with respect to the reference matching M_0 given on the right, have a $+$ sign in the expansion of $\det(K_1)$.

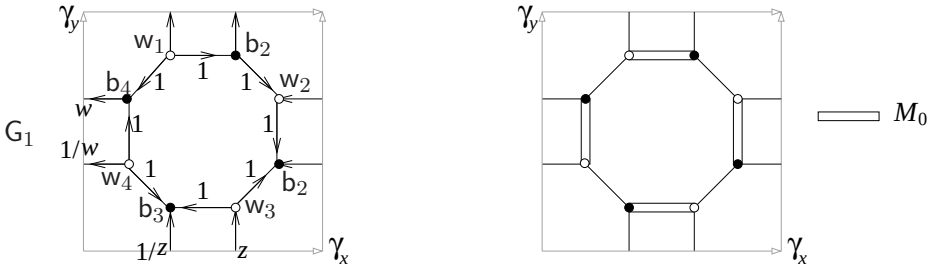

Figure 3.5: Left: labeling of the vertices of G_1, edge-weights of the altered Kasteleyn matrix, choice of admissible Kasteleyn orientation. Right: choice of reference perfect matching M_0.

The altered Kasteleyn matrix $K_1(z,w)$ is:

$$K_1(z,w) = \begin{pmatrix} 1 & 0 & \frac{1}{z} & 1 \\ -1 & 1 & 0 & -w \\ -z & 1 & 1 & 0 \\ 0 & \frac{1}{w} & 1 & 1 \end{pmatrix},$$

and the characteristic polynomial is:

$$P(z,w) = \det(K_1(z,w)) = 5 - z - \frac{1}{z} - w - \frac{1}{w}. \tag{3.4}$$

Let us compute the right hand side of Equation (3.3) explicitly. With our choice of reference matching M_0 of Figure 3.5 (right), the total flux of ω^{M_0} through γ_x and γ_y is $(0,0)$, so that $z^{x_0}w^{y_0} = 1$. Since all edges have weight 1, $\nu(M) \equiv 1$. Figure 3.6 describes the 9 perfect matchings of G_1, with their respective height change. As a consequence, the contribution of the perfect matchings of G_1 to the right hand side of (3.3) is 1 for each of the 5 first ones, $-w$, respectively, $-\frac{1}{w}$, $-z$, $-\frac{1}{z}$ for the last four ones. Combining the different contributions yields, as expected, the characteristic polynomial as computed in Equation (3.4).

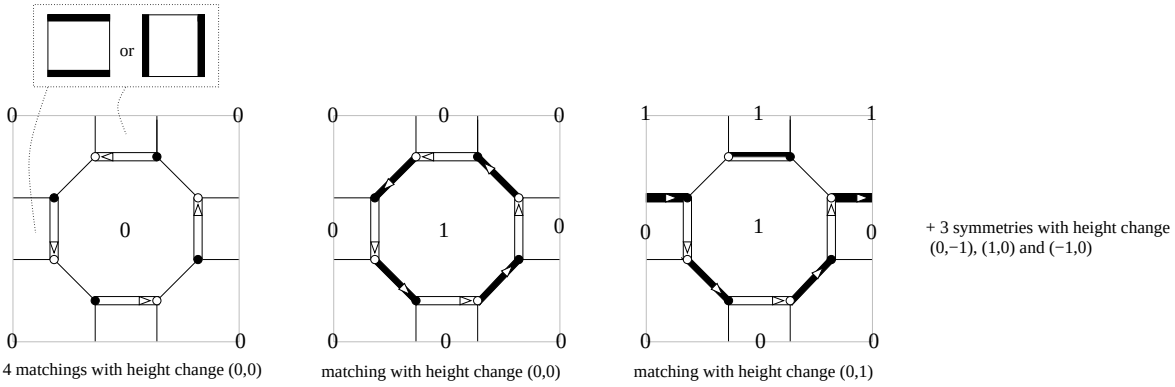

Figure 3.6: 9 possible dimer configurations of G_1 with their height change.

In the specific case when $(z,w) \in \{-1,1\}^2$ in $K_1(z,w)$, on recovers the four matrices $(K_1^{\theta\tau})_{\theta,\tau\in\{0,1\}}$. Using Equation (3.2), we recover that the number of dimer configurations of G_1 is:

$$Z(\mathsf{G}_1) = \frac{1}{2}\left(-P(1,1) + P(-1,1) + P(1,-1) + P(-1,-1)\right) = 9. \tag{3.5}$$

Characteristic polynomials of larger graphs may be computed recursively as follows. Let K_n be a Kasteleyn matrix of the graph G_n as above, and let $\gamma_{x,n}$ and $\gamma_{y,n}$ be the horizontal and vertical cycles of G_n^*. For $z,w \in \mathbb{C}$, the altered Kasteleyn matrix $K_n(z,w)$ is constructed similarly to $K_1(z,w)$, and the characteristic polynomial of G_n is $P_n(z,w) = \det(K_n(z,w))$.

Theorem 9. [CKP01, KOS06] *For every $n \geq 1$, and every $(z,w) \in \mathbb{C}^2$, the characteristic polynomial $P_n(z,w)$ of G_n is:*

$$P_n(z,w) = \prod_{\alpha_i^n = z} \prod_{\beta_j^n = w} P(\alpha_i, \beta_j).$$

Proof. The proof is a generalization of [CKP01] where the same result is obtained for the graph $\mathsf{G} = \mathbb{Z}^2$. We only give the argument when $z = w = 1$. The proof for general z,w's follows the same steps. Note that $K_n(1,1) = K_n^{00} = K_n$, so that our goal is to show that, for every $n \geq 1$:

$$\det(K_n) = \prod_{\alpha_i^n = 1} \prod_{\beta_j^n = 1} \det(K_1(\alpha_i, \beta_j)).$$

Let W_n, respectively B_n, denote the set of white, respectively black, vertices of G_n. The idea is to use the translation invariance of the graph G_n and of the matrix K_n to block diagonalize K_n, and to compute its determinant by computing the determinant of the different blocks.

Let $\mathbb{C}^{\mathsf{W}_n}$ be the set of complex-valued functions on white vertices W_n, and $\mathbb{C}^{\mathsf{B}_n}$ those on black vertices B_n. Then the matrix K_n can be interpreted as a linear operator from $\mathbb{C}^{\mathsf{B}_n}$ to $\mathbb{C}^{\mathsf{W}_n}$: let $f \in \mathbb{C}^{\mathsf{B}_n}$, then

$$(K_n f)(\mathsf{w}) = \sum_{\mathsf{b} \in \mathsf{B}_n} K_n(\mathsf{w}, \mathsf{b}) f(\mathsf{b}).$$

Let $T_x^{\mathsf{B}_n}$ (resp. $T_y^{\mathsf{B}_n}$) be the horizontal (resp. vertical) translation operator acting on $\mathbb{C}^{\mathsf{B}_n}$:

$$\forall \mathsf{b} \in \mathsf{B}_n, \quad (T_x^{\mathsf{B}_n} f)(\mathsf{b}) = f(\mathsf{b} + (1,0)), \quad (T_y^{\mathsf{B}_n} f)(\mathsf{b}) = f(\mathsf{b} + (0,1)),$$

and consider $T^{\mathsf{B}_n} = T_y^{\mathsf{B}_n} \circ T_x^{\mathsf{B}_n}$. The operator T^{B_n} being an isometry, it yields an orthonormal decomposition of $\mathbb{C}^{\mathsf{B}_n}$, consisting of eigenvectors of T^{B_n}. The eigenvalues of T^{B_n} are the products of n-th roots of unity: $(\alpha_j \beta_k)_{j,k \in \{0,\dots,n-1\}}$, where $\alpha_j = e^{i\frac{2\pi j}{n}}$, $\beta_k = e^{i\frac{2\pi k}{n}}$ (as a consequence of the fact that $(T^{\mathsf{B}_n})^n = \mathrm{Id}$). Let us denote by $V_{\alpha_j\beta_k}^{\mathsf{B}_n}$ the eigenspace of the eigenvalue $\alpha_j\beta_k$: $V_{\alpha_j\beta_k}^{\mathsf{B}_n} = \{f \in \mathbb{C}^{\mathsf{B}_n} : \forall \mathsf{b} \in \mathsf{B}_n,\, f(\mathsf{b} + (1,1)) = \alpha_j\beta_k f(\mathsf{b})\}$. Then $V_{\alpha_j\beta_k}^{\mathsf{B}_n}$ can be rewritten as $V_{\alpha_j\beta_k}^{\mathsf{B}_n} = \{f \in \mathbb{C}^{\mathsf{B}_n} : \forall \mathsf{b} \in \mathsf{B}_1, \forall (x,y) \in \{0,\dots,n-1\}^2, f(\mathsf{b} + (x,y)) = f(\mathsf{b})\alpha_j^x \beta_k^y\}$, where recall that $\mathsf{G}_1 = (\mathsf{W}_1 \cup \mathsf{B}_1, \mathsf{E}_1)$ is the fundamental domain. For every $\mathsf{b} \in \mathsf{B}_1$, define $\mathsf{e}_{\alpha_j\beta_k}^{\mathsf{b}} \in \mathbb{C}^{\mathsf{B}_n}$ by:

$$\forall\, \mathsf{b}' \in \mathsf{B}_1,\ \forall\, (x,y) \in \{0,\dots,n-1\}^2, \quad \mathsf{e}_{\alpha_j\beta_k}^{\mathsf{b}}(\mathsf{b}' + (x,y)) = \frac{1}{n}\delta_{\mathsf{b},\mathsf{b}'}\alpha_j^x\beta_k^y.$$

Then, $\mathsf{E}_{\alpha_j\beta_k} = \{\mathsf{e}_{\alpha_j\beta_k}^{\mathsf{b}} : \mathsf{b} \in \mathsf{B}_1\}$ is a basis of $V_{\alpha_j\beta_k}^{\mathsf{B}_n}$, the eigenspace $V_{\alpha_j\beta_k}^{\mathsf{B}_n}$ is $\frac{|V(\mathsf{G}_1)|}{2}$ dimensional, and $\mathsf{E} = \cup_{\{\alpha_j\beta_k : j,k \in \{0,\dots,n-1\}\}} \mathsf{E}_{\alpha_j\beta_k}$ is an orthonormal basis of $\mathbb{C}^{\mathsf{B}_n}$. In a similar way, one obtains an orthonormal decomposition of $\mathbb{C}^{\mathsf{W}_n}$ using $T^{\mathsf{W}_n} = T_x^{\mathsf{W}_n} \circ T_y^{\mathsf{W}_n}$ acting on $\mathbb{C}^{\mathsf{W}_n}$.

Let us show that K_n represented in this basis is block diagonal, with a block of size $\frac{|V(\mathsf{G}_1)|}{2}$ for each of the n^2 eigenvalues $\alpha_j\beta_k$. For all $\mathsf{w} \in \mathsf{W}_1$, $(x,y) \in \{0,\dots,n-1\}^2$, one has:

$$\begin{aligned}
(K_n \mathsf{e}_{\alpha_j\beta_k}^{\mathsf{b}})(\mathsf{w} + (x,y)) &= \sum_{\mathsf{b}' \in \mathsf{B}_1} \sum_{(x',y') \in \{0,\dots,n-1\}^2} K_n(\mathsf{w} + (x,y), \mathsf{b}' + (x',y')) \mathsf{e}_{\alpha_j\beta_k}^{\mathsf{b}}(\mathsf{b}' + (x'+y')) \\
&= \sum_{(x',y') \in \{0,\dots,n-1\}^2} K_n(\mathsf{w} + (x,y), \mathsf{b} + (x',y')) \frac{1}{n} \alpha_j^{x'} \beta_k^{y'}, \text{ by definition of } \mathsf{e}_{\alpha_j\beta_k}^{\mathsf{b}} \\
&= \frac{1}{n} K_1(\alpha_j, \beta_k)_{\mathsf{w},\mathsf{b}}\, \alpha_j^x \beta_k^y, \text{ by translation invariance of } K_n \\
&= \sum_{\mathsf{w}' \in \mathsf{W}_1} K_1(\alpha_j, \beta_k)_{\mathsf{w}',\mathsf{b}}\, \mathsf{e}_{\alpha_j\beta_k}^{\mathsf{w}'}(\mathsf{w} + (x,y)), \text{ by definition of } \mathsf{e}_{\alpha_j\beta_k}^{\mathsf{w}'}.
\end{aligned}$$

As a consequence, $(K_n \mathsf{e}_{\alpha_j\beta_k}^{\mathsf{b}}) \in V_{\alpha_j\beta_k}^{\mathsf{W}_n}$, and the matrix K_n written in the basis E is block diagonal. For all $\mathsf{w} \in \mathsf{W}_1$, $\mathsf{b} \in \mathsf{B}_1$, the (w,b)- coefficient of the block corresponding to the eigenvalue $\alpha_j\beta_k$ is given by:

$$\begin{aligned}
(\mathsf{e}_{\alpha_j\beta_k}^{\mathsf{w}})^* K_n \mathsf{e}_{\alpha_j\beta_k}^{\mathsf{b}} &= \sum_{\mathsf{w}' \in \mathsf{W}_1} K_1(\alpha_j, \beta_k)_{\mathsf{w}',\mathsf{b}}\, (\mathsf{e}_{\alpha_j\beta_k}^{\mathsf{w}})^*\, \mathsf{e}_{\alpha_j\beta_k}^{\mathsf{w}'} \\
&= K_1(\alpha_j, \beta_k)_{\mathsf{w},\mathsf{b}}, \text{ since the basis is orthonormal,}
\end{aligned}$$

thus proving Theorem 9 in the case where $z = w = 1$. □

3.2.3 Free energy

As a corollary to Theorems 7 and 9, we have an explicit expression for the partition function of G_n as a function of the characteristic polynomial P.

Corollary 10. *When the Kasteleyn orientation is chosen such that the sign table of the fundamental domain is given by Table 3.1, then for every $n \geq 1$,*

$$Z(\mathsf{G}_n) = \frac{1}{2}\left(-Z_n^{00} + Z_n^{10} + Z_n^{01} + Z_n^{11}\right),$$

where $Z_n^{\theta\tau} = P_n((-1)^\theta, (-1)^\tau) = \prod_{\alpha_i^n=(-1)^\theta} \prod_{\beta_j^n=(-1)^\tau} P(\alpha_i, \beta_j)$.

The partition function is growing with the size of the graph. A natural question to ask now is : "what is this growth rate ?" In order to formulate the question correctly, we need to know about the order of magnitude of this growth. Intuition tells us that it is going to be exponential in the area of the graph: $Z(\mathsf{G}_n) \sim e^{cn^2}$. Thus the right quantity to look at is:

$$\lim_{n\to\infty} \frac{1}{n^2} \log Z(\mathsf{G}_n).$$

Minus this quantity is known as the *free energy*.

Theorem 11. [CKP01, KOS06] *Under the assumption that $P(z, w)$ has only a finite number of zeros on the unit torus $\mathbb{T}^2 = \{(z, w) \in \mathbb{C}^2 : |z| = |w| = 1\}$, we have:*

$$\lim_{n\to\infty} \frac{1}{n^2} \log Z(\mathsf{G}_n) = \frac{1}{(2\pi i)^2} \int_{\mathbb{T}^2} \log|P(z, w)| \frac{dz}{z} \frac{dw}{w}.$$

Proof. Since $Z_n^{\theta\tau}$ counts some dimer configurations of G_n with the wrong sign, we have the following bound:

$$Z_n^{\theta\tau} \leq Z(\mathsf{G}_n).$$

Moreover, looking at Table 3.1, we deduce:

$$-Z_n^{00} \leq +Z_n^{10} + Z_n^{01} + Z_n^{11},$$

and thus by Theorem 7,

$$\max_{\theta,\tau\in\{0,1\}} \{Z_n^{\theta\tau}\} \leq Z(\mathsf{G}_n) \leq Z_n^{10} + Z_n^{01} + Z_n^{11} \leq 3 \max_{\theta,\tau\in\{0,1\}} \{Z_n^{\theta\tau}\}.$$

So that $\lim_{n\to\infty} \frac{1}{n^2} \log Z(\mathsf{G}_n) = \lim_{n\to\infty} \frac{1}{n^2} \log\left(\max_{\theta,\tau\in\{0,1\}} \{Z_n^{\theta\tau}\}\right)$, provided that these limits exist. By Theorem 9, we have:

$$\frac{1}{n^2} \log Z_n^{00} = \frac{1}{(2\pi)^2} \frac{(2\pi)^2}{n^2} \sum_{j=0}^{n-1} \sum_{k=0}^{n-1} \log P(e^{i\frac{2\pi j}{n}}, e^{i\frac{2\pi k}{n}}). \tag{3.6}$$

The other terms $\frac{1}{n^2} \log Z_n^{\theta\tau}$ can be written in a similar way. These four terms look like Riemann sums for the integral:

$$I = \frac{1}{(2\pi)^2} \int_0^{2\pi} \int_0^{2\pi} \log P(e^{i\theta}, e^{i\tau}) d\theta\, d\tau = \frac{1}{(2\pi i)^2} \int_{\mathbb{T}^2} \log P(z, w) \frac{dz}{z} \frac{dw}{w}.$$

We may nevertheless have a convergence problem. Indeed, terms of the sum (3.6) with arguments too close to the zeros of $P(z,w)$ may explode. By using the very careful argument of Theorem 7.3. of [CKP01], one can check that this will not happen, and so the Riemann sum of the maximum converges to the integral I.

The proof is concluded by observing that since $P(e^{-i\theta}, e^{-i\tau}) = \overline{P(e^{i\theta}, e^{i\tau})}$,

$$I = \frac{1}{(2\pi)^2} \int_0^{2\pi} \int_0^{2\pi} \log |P(e^{i\theta}, e^{i\tau})| d\theta \, d\tau.$$

□

Example. The free energy of the dimer model on the square-octagon graph with uniform weights is:

$$-\frac{1}{(2\pi i)^2} \int_{\mathbb{T}^2} \log \left| 5 - z - \frac{1}{z} - w - \frac{1}{w} \right| \frac{dz}{z} \frac{dw}{w}.$$

Note that it is in general hard to explicitly compute this integral.

3.3 Gibbs measures

We are now interested in characterizing probability measures on the set of perfect matchings $\mathcal{M}(\mathsf{G})$ of the infinite graph G which are, in some appropriate sense, infinite volume versions of the Boltzmann measure on $\mathcal{M}(\mathsf{G}_n)$. Recall that by definition, the probability of a matching chosen with respect to the Boltzmann measure on $\mathcal{M}(\mathsf{G}_n)$ is proportional to the product of its edge weights. This definition does not work when the graph is infinite, and is replaced by the notion of *Gibbs measure*, which is a probability measure on $\mathcal{M}(\mathsf{G})$ satisfying the DLR [1] conditions: if the perfect matching in an annular region of G is fixed, matchings inside and outside of the annulus are independent, and the probability of any interior matching is proportional to the product of its edge-weights.

3.3.1 Limit of Boltzmann measures

A natural way of constructing a Gibbs measure is to take the limit of the Boltzmann measures on *cylinder sets* of $\mathcal{M}(\mathsf{G}_n)$, where a cylinder set consists of all perfect matchings containing a fixed subset of edges of G_n.

Theorem 2 gives an explicit expression for the Boltzmann measure on cylinder sets when the graph is planar and finite. In the case of toroidal graphs, a similar but more complicated expression holds: it is a combination of fours terms similar to those of Equation (2.2), involving the matrices $K_n^{00}, \ldots, K_n^{11}$, and their inverses.

Using the block diagonalization of the matrices $K_n^{\sigma\tau}$ of the proof of Theorem 9, one can compute the elements of the inverse explicitly and obtain Riemann sums. The convergence of these Riemann sums is again complicated by the zeros of $P(z,w)$ on the torus $\mathbb{T}^2$, but can be shown to converge on a subsequence of n's to the right hand side of Equation (3.7). Using a Theorem of Sheffield [She05] which shows a priori existence of the limit, one deduces convergence for every n. Then, by Kolmogorov's extension theorem, there exists a unique probability measure on $(\mathcal{M}(\mathsf{G}), \sigma(\mathcal{A}))$ which coincides with the limit of the Boltzmann measures on cylinder sets, where $\sigma(\mathcal{A})$ is the smallest sigma-field containing cylinder sets. This limiting measure is of Gibbs type by construction. We have thus sketched the proof of the following theorem.

[1] DLR stands for Dobrushin, Lanford and Ruelle

Theorem 12. [CKP01, KOS06] *Let* $\{\mathsf{e}_1 = \mathsf{w}_1\mathsf{b}_1, \dots, \mathsf{e}_k = \mathsf{w}_k\mathsf{b}_k\}$ *be a subset of edges of* G. *Then there exists a unique probability measure* μ *on* $(\mathcal{M}(\mathsf{G}), \sigma(\mathcal{A}))$ *such that:*

$$\mu(\mathsf{e}_1, \dots, \mathsf{e}_k) = \left(\prod_{i=1}^{k} K(\mathsf{w}_i, \mathsf{b}_i)\right) \det(K^{-1}(\mathsf{b}_i, \mathsf{w}_j)_{1\le i,j\le k}), \tag{3.7}$$

where K *is a Kasteleyn matrix associated to the graph* G, *and assuming* b *and* w *are in a single fundamental domain:*

$$K^{-1}(\mathsf{b}, \mathsf{w} + (x, y)) = \frac{1}{(2\pi i)^2} \int_{\mathbb{T}^2} \frac{Q_{\mathsf{bw}}(z, w)}{P(z, w)} z^x w^y \frac{dw}{w} \frac{dz}{z},$$

and $Q_{\mathsf{bw}}(z, w)$ *is the* (b, w) *element of the adjugate matrix (transpose of the cofactor matrix) of* $K_1(z, w)$. *It is a polynomial in* z, w, z^{-1}, w^{-1}.

3.3.2 Ergodic Gibbs measures

In the previous section, we have explicitly determined a Gibbs measure on $\mathcal{M}(\mathsf{G})$. We now aim at characterizing all of them. In order to this in a way which is coherent with the model, we introduce the following notions.

A probability measure on $\mathcal{M}(\mathsf{G})$ is *translation-invariant*, if the measure of a subset of $\mathcal{M}(\mathsf{G})$ is invariant under the translation-isomorphism action. An *ergodic Gibbs measure* (EGM) is a Gibbs measure which is translation invariant and ergodic, *i.e.* translation invariant sets have measure 0 or 1.

For an ergodic Gibbs measure μ, define the *slope* (s, t) to be the expected horizontal and vertical height change in the $(1, 0)$ and $(0, 1)$ directions, that is $s = \mathbb{E}_\mu[h(\mathsf{v} + (1, 0)) - h(\mathsf{v})]$, and $t = \mathbb{E}_\mu[h(\mathsf{v} + (0, 1)) - h(\mathsf{v})]$.

Let us denote by μ_n the Boltzmann measure on $\mathcal{M}(\mathsf{G}_n)$. For a fixed $(s, t) \in \mathbb{R}^2$, let $\mathcal{M}_{s,t}(\mathsf{G}_n)$ be the set of matchings of G_n which have height change $(\lfloor sn \rfloor, \lfloor tn \rfloor)$. Assuming that $\mathcal{M}_{s,t}(\mathsf{G}_n)$ is non-empty for n sufficiently large, let $\mu_n(s, t)$ denote the conditional measure induced by μ_n on $\mathcal{M}_{s,t}(\mathsf{G}_n)$. Then, a characterization of all ergodic Gibbs measures on $\mathcal{M}(\mathsf{G})$ is given by the following theorem of Sheffield.

Theorem 13. [She05] *For each* (s, t) *for which* $\mathcal{M}_{s,t}(\mathsf{G}_n)$ *is non-empty for* n *sufficiently large,* $\mu_n(s, t)$ *converges as* $n \to \infty$ *to an EGM* $\mu(s, t)$ *of slope* (s, t). *Furthermore* μ_n *itself converges to* $\mu(s_0, t_0)$ *where* (s_0, t_0) *is the limit of the slopes of* μ_n. *Finally, if* (s_0, t_0) *lies in the interior of the set of* (s, t) *for which* $\mathcal{M}_{s,t}(\mathsf{G}_n)$ *is non-empty for* n *sufficiently large, then every EGM of slope* (s, t) *is of the form* $\mu(s, t)$ *for some* (s, t) *as above; that is* $\mu(s, t)$ *is the unique ergodic Gibbs measure of slope* (s, t).

Proof. The existence is established by taking limits of Boltzmann measures on larger and larger tori while restricting height change. The uniqueness is much harder, and we won't discuss it here. □

3.3.3 Newton polygon and available slopes

Theorem 13 raises the following question: what is the set of possible slopes for Gibbs measures or equivalently for limits of conditional Boltzmann measures ? The answer is given by the *Newton polygon* $N(P)$ defined as follows: $N(P)$ is the closed convex hull in $\mathbb{R}^2$ of the set of integer

exponents of the monomials of the characteristic polynomial $P(z,w)$, up to contribution of the reference flow ω^{M_0}, that is:

$$N(P) = \text{convex hull}\{(i,j) \in \mathbb{Z}^2 | z^{i+x_0} w^{j+y_0} \text{ is a monomial in } P(z,w)\}.$$

Proposition 14. [KOS06] *The Newton polygon is the set of possible slopes of EGMs, that is there exists an EGM $\mu(s,t)$ if and only if $(s,t) \in N(P)$.*

Proof. Observing that changing the reference flow merely translates the Newton polygon, we assume that $(x_0, y_0) = (0,0)$.

Let us first prove that if $(s,t) \in N(P)$, then there is a Gibbs measure of slope (s,t), or equivalently $\mathcal{M}_{s,t}(\mathsf{G}_n)$ is non-empty for n large enough. For convenience, we will assume that the set of possible slopes is closed.

By Lemma 8, the absolute value of the coefficient $z^i w^j$ in $P(z,w)$ is the weighted sum of matchings of G_1 with height change (i,j), thus there is a matching corresponding to each extremal point of $N(P)$, *i.e.* if (s,t) is an extremal point of $N(P)$, then $\mathcal{M}_{s,t}(\mathsf{G}_1) \neq \emptyset$. It suffices to show that if $\mathcal{M}_{s_1,t_1}(\mathsf{G}_{n_1})$ and $\mathcal{M}_{s_2,t_2}(\mathsf{G}_{n_2})$ are non-empty for some n_1 and n_2, then $\mathcal{M}_{\frac{s_1+s_2}{2},\frac{t_1+t_2}{2}}(\mathsf{G}_m)$ is also non-empty for some m. Indeed, by induction, this allows to prove existence of a Gibbs measure of slope (s,t) for a dense subset of the Newton polygon. The proof is ended by using the assumption that the set of possible slopes is closed.

Without loss of generality, we can assume that $n_1 = n_2$, otherwise take the lcm of their periods. Consider two matchings of $\mathcal{M}_{s_1,t_1}(\mathsf{G}_n)$ and $\mathcal{M}_{s_2,t_2}(\mathsf{G}_n)$, respectively. The superimposition of the two matchings being a set of disjoint alternating cycles, one can change from one matching to the other by rotating along the cycles. If the height changes $(\lfloor s_1 n \rfloor, \lfloor t_1 n \rfloor)$, $(\lfloor s_2 n \rfloor, \lfloor t_2 n \rfloor)$ of the two matchings are unequal, some of these cycles have non-zero homology in $H_1(\mathbb{T}^2, \mathbb{Z})$, so that rotating along them will change the height change. On the toroidal graph G_{2n}, consider four copies of the two matchings and shift half of the non-trivial cycles; this creates a new matching with height change $(\lfloor (s_1+s_2)n \rfloor, \lfloor (t_1+t_2)n \rfloor) = \left(\lfloor \frac{s_1+s_2}{2}\, 2n \rfloor, \lfloor \frac{t_1+t_2}{2}\, 2n \rfloor\right)$, thus proving that $\mathcal{M}_{\frac{s_1+s_2}{2},\frac{t_1+t_2}{2}}(\mathsf{G}_m)$ is non-empty for $m = 2n$.

Let us now suppose that there exists a Gibbs measure $\mu(s,t)$ of slope (s,t) and prove that $(s,t) \in N(P)$. Denote by $\vec{\mathsf{E}}_1$ the set of directed edges of the fundamental domain $\mathsf{G}_1 = (\mathsf{V}_1, \mathsf{E}_1)$. Recalling that the divergence div is a linear function of flows, the set of non-negative, white-to-black unit flows defines a polytope of $\mathbb{R}^{\vec{\mathsf{E}}_1}$:

$$\{\omega \in \mathbb{R}^{\vec{\mathsf{E}}_1} : \forall\, \mathsf{wb} \in \mathsf{E}_1,\, \omega(\mathsf{b},\mathsf{w}) = 0,\, 0 \leq \omega(\mathsf{w},\mathsf{b}) \leq 1;\, \forall\, \mathsf{w} \in \mathsf{W}_1,\, \operatorname{div}\omega(\mathsf{w}) = 1,\, \forall\, \mathsf{b} \in \mathsf{B}_1,\, \operatorname{div}\omega(\mathsf{b}) = -1\}.$$

The mapping ψ which assigns to a flow ω the total flux across γ_x and γ_y is a linear mapping from the polytope to $\mathbb{R}^2$, implying that the image of the polytope under ψ is the convex hull of the images of the extremal points of the polytope.

Now, from Section 3.1, we know that every dimer configuration of G_1 defines a non-negative, white-to-black unit flow taking values in $\{0,1\}$ on every directed edge of $\vec{\mathsf{E}}_1$. The converse being also true, this implies that extremal points of the polytope are given by dimer configurations. Since the reference flow is such that $(x_0, y_0) = (0,0)$, the image of a dimer configuration under ψ is its height change. This means that the image of extremal points of the polytope contains the extremal points of the Newton polygon $N(P)$; the image of the polytope under ψ is thus $N(P)$.

The Gibbs measure $\mu(s,t)$ of slope (s,t) defines a non-negative, white-to-black flow $\omega^{\mu(s,t)}$:

$$\forall\, \mathsf{e} = \mathsf{wb} \in \mathsf{E}_1,\, \omega^{\mu(s,t)}(\mathsf{w},\mathsf{b}) = \mu(s,t)(\mathsf{e}),\, \omega^{\mu(s,t)}(\mathsf{b},\mathsf{w}) = 0.$$

Since $\mu(s,t)$ is a probability measure, the flow $\omega^{\mu(s,t)}$ has divergence 1 at every white vertex and -1 at every black vertex. It thus belongs to the polytope and its image under ψ belongs to $N(P)$. The proof is concluded by observing that the image of $\mu(s,t)$ under ψ is the slope (s,t). □

Example 3.2. Figure 3.7 shows the Newton polygon of the dimer model on the square-octagon graph with weights 1 on the edges. Marked points represent monomials of the characteristic polynomial $P(z,w) = 5 - z - \frac{1}{z} - w - \frac{1}{w}$.

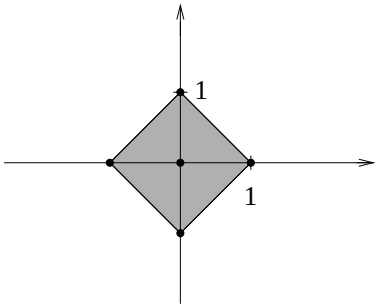

Figure 3.7: Newton polygon of the dimer model on the square-octagon graph with uniform weights.

3.3.4 Surface tension

For every $(s,t) \in N(P)$, let $Z_{s,t}(\mathsf{G}_n)$ be the partition function of $\mathcal{M}_{s,t}(\mathsf{G}_n)$, that is:

$$Z_{s,t}(\mathsf{G}_n) = \sum_{M \in \mathcal{M}_{s,t}(\mathsf{G}_n)} \nu(M).$$

Then, by definition, the *free energy* of the measure $\mu(s,t)$ is:

$$\sigma(s,t) = -\lim_{n\to\infty} \frac{1}{n^2} \log Z_{s,t}(\mathsf{G}_n).$$

The function $\sigma : N(P) \to \mathbb{R}$ is known as the *surface tension*. Sheffield [She05] proves that it is strictly convex.

As a consequence of this definition and of Theorem 13, one deduces that the measure $\mu(s_0,t_0)$ of Theorem 13 is the one which has minimal free energy. Moreover, since the surface tension is strictly convex, the surface tension minimizing slope is unique and equal to (s_0,t_0).

3.3.5 Constructing Gibbs measures

Theorem 12 of Section 3.3.1 proves an explicit expression for the Gibbs measure $\mu(s_0,t_0)$ of slope (s_0,t_0). Our goal now is to obtain an explicit expression for the Gibbs measures $\mu(s,t)$ with all possible slopes (s,t).

Recall that by Theorem 13, the Gibbs measure $\mu(s,t)$ is the limit of the conditional Boltzmann measures $\mu_n(s,t)$ on $\mathcal{M}_{s,t}(\mathsf{G}_n)$. The problem is that conditional measures are hard objects to work with in order to obtain explicit expressions. But we know how to handle the full Boltzmann measure, which converges to the Gibbs measure of slope (s_0,t_0). So the idea to avoid handling conditional measures is to modify the weight function on the edges of G_n in such

a way that matchings with another slope than (s_0, t_0) get favored. Hence, we are looking for a weight function which satisfies the following: the new weight of a matching is equal to the old weight multiplied by a quantity which depends only on its height change. This can be done by introducing *magnetic field coordinates* as follows.

Recall that $\gamma_{x,n}$, $\gamma_{y,n}$ are oriented horizontal and vertical cycles in the dual graph G_n^* obtained by taking n times the basis vector e_x of the underlying lattice $\mathbb{Z}^2$, n times the basis vector e_y respectively, embedded on the torus. Then, on G_n^* there are n horizontal copies of the cycle $\gamma_{x,n}$, and n vertical copies of the cycle $\gamma_{y,n}$. Let (B_x, B_y) be two real numbers known as *magnetic field coordinates*. Multiply all edges crossing the n copies of the horizontal cycle $\gamma_{x,n}$ by $e^{\pm B_x}$, depending on whether the white vertex is on the left or on the right. In a similar way, edges crossing the n copies of the vertical cycle $\gamma_{y,n}$ are multiplied by $e^{\pm B_y}$. This defines a *magnetic altered weight function*, denoted by $\nu_{(B_x,B_y)}$ satisfying our requirement. Indeed, let M_0 be the periodic reference matching of G_n, and denote by x_0^n, y_0^n the total flux of ω^{M_0} through $\gamma_{x,n}$, $\gamma_{y,n}$. Then, arguing in a way similar to the proof of Lemma 8, one can express the magnetic altered weight function $\nu_{(B_x,B_y)}$ as the weight function ν, multiplied by a quantity which only depends on the height change:

$$\forall\, M \in \mathcal{M}(\mathsf{G}_n), \quad \nu_{(B_x,B_y)}(M) = \nu(M) e^{nB_x(h_x^M + x_0^n)} e^{nB_y(h_y^M + y_0^n)}. \tag{3.8}$$

Let $P_{(B_x,B_y)}(z,w)$ be the characteristic polynomial of the graph G_1 corresponding to the magnetic altered weight function. The key fact is that $P_{(B_x,B_y)}(z,w)$ can easily be expressed using the characteristic polynomial $P(z,w)$ of the graph G_1: expressing $P_{(B_x,B_y)}(z,w)$ using Lemma 8 and replacing $\nu_{(B_x,B_y)}(M)$ by the right hand side of (3.8) in the case where $n=1$, yields:

$$P_{(B_x,B_y)}(z,w) = P(e^{B_x} z, e^{B_y} w).$$

Let $Z_{(B_x,B_y)}(\mathsf{G}_n)$ be the partition function and $\mu_n^{(B_x,B_y)}$ be the Boltzmann measure of the graph G_n with the magnetic altered weight function. Denote by $\mu_{(B_x,B_y)}$ the Gibbs measure obtained as weak limit of the Boltzmann measures $\mu_n^{(B_x,B_y)}$. Then, as a direct corollary of Theorems 11 and 12, we have:

Corollary 15. [KOS06]
Under the assumption that $P(e^{B_x} z, e^{B_y} w)$ has only a finite number of zeros on the unit torus $\mathbb{T}^2$:

$$\lim_{n\to\infty} \frac{1}{n^2} \log Z_{(B_x,B_y)}(\mathsf{G}_n) = \frac{1}{(2\pi i)^2} \int_{\mathbb{T}^2} \log \left| P(e^{B_x} z, e^{B_y} w) \right| \frac{dz}{z} \frac{dw}{w}.$$

Corollary 16. [KOS06]
Let $\{\mathsf{e}_1 = \mathsf{w}_1\mathsf{b}_1, \ldots, \mathsf{e}_k = \mathsf{w}_k\mathsf{b}_k\}$ be a subset of edges of G. Then there exists a unique probability measure $\mu_{(B_x,B_y)}$ on $(\mathcal{M}(\mathsf{G}), \sigma(\mathcal{A}))$ such that:

$$\mu_{(B_x,B_y)}(\mathsf{e}_1, \ldots, \mathsf{e}_k) = \left(\prod_{i=1}^{k} K_{(B_x,B_y)}(\mathsf{w}_i, \mathsf{b}_i) \right) \det(K^{-1}_{(B_x,B_y)}(\mathsf{b}_i, \mathsf{w}_j)_{1\le i,j\le k}), \tag{3.9}$$

where $K_{(B_x,B_y)}$ is a Kasteleyn matrix associated to the graph G, and assuming b and w are in a single fundamental domain:

$$K^{-1}_{(B_x,B_y)}(\mathsf{b}, \mathsf{w} + (x,y)) = \frac{1}{(2\pi i)^2} \int_{\mathbb{T}^2} \frac{Q_{\mathsf{bw}}(e^{B_x} z, e^{B_y} w)}{P(e^{B_x} z, e^{B_y} w)} z^y w^{-x} \frac{dw}{w} \frac{dz}{z},$$

and $Q_{\mathsf{bw}}(z,w)$ is the (b,w) element of the adjugate matrix of $K_1(z,w)$ of the original graph.

So, it is quite remarkable that the results obtained for the weight function ν also yield the results for the magnetic altered weight function $\nu_{(B_x,B_y)}$.

Note that we have not yet related the magnetic field coordinates to the slope of the Gibbs measure $\mu_{(B_x,B_y)}$. This is postponed until Section 3.4.2.

3.4 Phases of the model

In this section, we describe one of the most beautiful results on the bipartite dimer model obtained by Kenyon, Okounkov and Sheffield [KOS06], namely the full description of the phase diagram of the dimer model. It involves magnetic field coordinates and an object from algebraic geometry called "Harnack curves".

A way to characterize phases is by the rate of decay of edge-edge correlations. In the dimer model, this amounts to studying asymptotics of $K^{-1}_{(B_x,B_y)}$. Indeed, let $\mathsf{e}_1 = \mathsf{w}_1\mathsf{b}_1$ and $\mathsf{e}_2 = \mathsf{w}_2\mathsf{b}_2$ be two edges of G, which are thought of as being far away from each other. Let $\mathbb{I}_e$ be the random variable which is 1 if the edge e is present in a dimer configuration, and 0 else. Then, using the explicit expression for the Gibbs measure $\mu_{(B_x,B_y)}$ yields:

$$\begin{aligned}\mathrm{Cov}(\mathbb{I}_{\mathsf{e}_1}, \mathbb{I}_{\mathsf{e}_2}) &= \mu_{(B_x,B_y)}(\mathsf{e}_1,\mathsf{e}_2) - \mu_{(B_x,B_y)}(\mathsf{e}_1)\mu_{(B_x,B_y)}(\mathsf{e}_2),\\ &= K_{(B_x,B_y)}(\mathsf{w}_1,\mathsf{b}_1)K_{(B_x,B_y)}(\mathsf{w}_2,\mathsf{b}_2)K^{-1}_{(B_x,B_y)}(\mathsf{b}_2,\mathsf{w}_1)K^{-1}_{(B_x,B_y)}(\mathsf{b}_1,\mathsf{w}_2).\end{aligned}$$

The asymptotic behavior of $K^{-1}_{(B_x,B_y)}(\mathsf{b},\mathsf{w}+(x,y))$ (as x^2+y^2 gets large) depends on the zeros of the denominator on the unit torus, *i.e.* on the zeros of $P(e^{B_x}z, e^{B_y}w)$ on the unit torus. Hence, the goal is to study the set: $\{(z,w)\in\mathbb{T}^2 \,:\, P(e^{B_x}z,e^{B_y}w)=0\}$, or equivalently, the set:

$$\{(z,w)\in\mathbb{C}^2 \,:\, |z|=e^{B_x},\, |w|=e^{B_y},\, P(z,w)=0\}.$$

This is the subject of the next section.

3.4.1 Amoebas, Harnack curves and Ronkin function

The *amoeba* of a polynomial $P\in\mathbb{C}[z,w]$ in two complex variables, denoted by $\mathbb{A}(P)$, is defined as the image of the curve $P(z,w)=0$ in $\mathbb{C}^2$ under the map:

$$(z,w)\mapsto(\log|z|,\log|w|).$$

When P is the characteristic polynomial of a dimer model, the curve $P(z,w)=0$ is known as the *spectral curve of the dimer model*. Note that a point $(x,y)\in\mathbb{R}^2$ is in the amoeba $\mathbb{A}(P)$, if and only if $|z|=e^x$, $|w|=e^y$, and $P(z,w)=0$. Otherwise stated, a point $(x,y)\in\mathbb{R}^2$ is in the amoeba if and only if the polynomial $P(e^xz,e^yw)$ has at least one zero on the unit torus.

The theory of amoebas is a fresh and beautiful field of research. The paper "What is ... an amoeba?" in the notices of the AMS, by Oleg Viro gives a very nice overview of the results obtained over a period of 8 years by [FPT00, GKZ94, Mik00, MR01]. It provides a precise geometric picture of the object, which heavily depends on the Newton polygon $N(P)$ of Section 3.3.3. Loosely stated, an amoeba satisfies the following, see also Figure 3.8.

- An amoeba reaches infinity by several tentacles. Each tentacle accommodates a ray and narrows exponentially fast towards it, so that there is only one ray in each tentacle.

- Each ray is orthogonal to a side of the Newton polygon $N(P)$, and directed towards an outward normal of the side.
- For each side of $N(P)$, there is at least one tentacle associated to it. The maximal number of tentacles corresponding to a side of $N(P)$ is the number of pieces it is divided in by integer lattice points.
- The amoeba's complement $\mathbb{R}^2 \setminus \mathbb{A}(P)$ consists of components between the tentacles, and bounded components. Each bounded component corresponds to a different integer lattice point of $N(P)$, and the maximal number of bounded components is the total number of interior integer lattice points of $N(P)$.
- Each connected component of the amoeba's complement $\mathbb{R}^2 \setminus \mathbb{A}(P)$ is convex.
- Planar amoebas are not bounded, but

$$\text{Area}(\mathbb{A}(P)) \leq \pi^2 \text{Area}(N(P)).$$

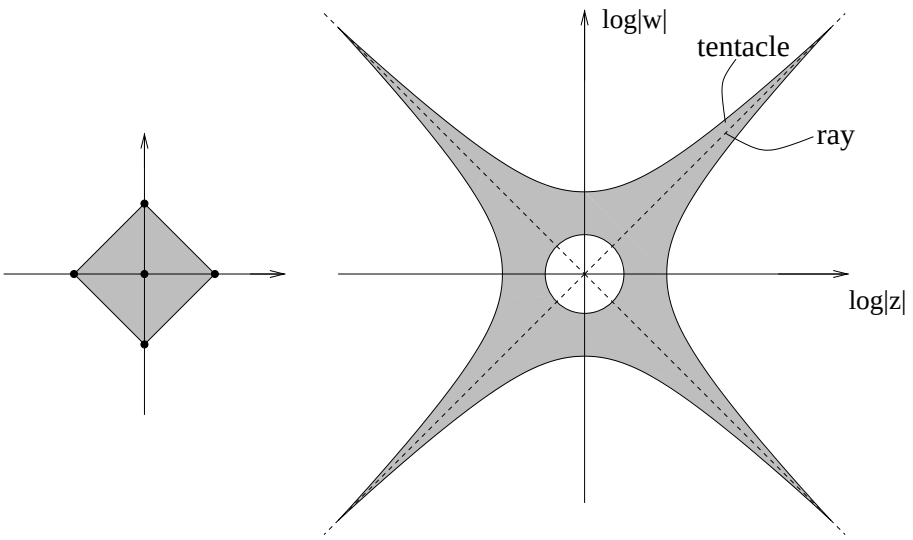

Figure 3.8: Newton polygon (left) and amoeba (right, shaded) of the characteristic polynomial $P(z,w) = 5 - z - \frac{1}{z} - w - \frac{1}{w}$ of the uniform dimer model on the square-octagon graph.

One of the main tools used to study the amoeba of a polynomial P is the Ronkin function R of this polynomial defined by:

$$\forall\,(x,y) \in \mathbb{R}^2, \quad R(x,y) = \frac{1}{(2\pi i)^2} \int_{\mathbb{T}^2} \log|P(e^x z, e^y w)| \frac{dz}{z} \frac{dw}{w}.$$

It has the following properties:

- The Ronkin function is convex
- It is linear on each component of the amoeba complement, and the gradient is the corresponding integer point of $N(P)$.

Complex curves $P(z,w)=0$ whose amoeba area is maximal, *i.e.* equal to $\pi^2\,\mathrm{Area}(N(P))$, are called *maximal*. Curves with this property are very special: they have real coefficients and their amoeba has the maximal number of components. Such curves were already introduced by Harnack in 1876, and are known as *Harnack curves*. There is an alternative characterization of Harnack curves given in [MR01], which is more useful here: a real curve $P(z,w)=0$ is Harnack if and only if the map from the curve to its amoeba is at most 2-to-1. It will be 2-to-1, with a finite number of possible exceptions where it may be 1-to-1 (the boundary of the amoeba, and when bounded components shrink to a point).

One of the most fruitful theorem of the paper [KOS06] is the following.

Theorem 17. [KOS06, KO06] *The spectral curve of a dimer model is a Harnack curve. Conversely, every Harnack curve arises as the spectral curve of some periodic bipartite weighted dimer model.*

For the proof of this theorem, we refer to [KOS06, KO06].

3.4.2 Surface tension revisited

In this section, we relate the magnetic field coordinates to the slope of the measure $\mu_{(B_x,B_y)}$. This is done by expressing the surface tension as a function of the Ronkin function.

Let us assume that the reference flow ω^{M_0} of the fundamental domain G_1 flows by 0 through the paths γ_x, γ_y, *i.e.* $x_0=y_0=0$.

Theorem 18. [KOS06] *The surface tension is the Legendre transform of the Ronkin function of the characteristic polynomial,* i.e.

$$\sigma(s,t)=\max_{x,y}\{-R(x,y)+sx+ty\}.$$

Proof. (Sketch) Let us sketch the proof that the Ronkin function is the Legendre transform of the surface tension. Since the surface tension is strictly convex [She05], then the Legendre transform is involutive, and Theorem 18 is obtained.

By Corollary 15, we know that:

$$R(B_x,B_y)=\lim_{n\to\infty}\frac{1}{n^2}\log Z_{(B_x,B_y)}(\mathsf{G}_n).$$

Moreover, by definition:

$$\begin{aligned}
Z_{(B_x,B_y)}(\mathsf{G}_n)&=\sum_{M\in\mathcal{M}(\mathsf{G}_n)}\nu(M)e^{nB_xh_x}e^{nB_yh_y}.\quad\text{This sum can be decomposed as:}\\
Z_{(B_x,B_y)}(\mathsf{G}_n)&=\iint_{N(P)}\sum_{\{M\in\mathcal{M}(\mathsf{G}_n):h_x=\lfloor ns\rfloor,h_y=\lfloor nt\rfloor\}}\nu(M)e^{nB_xh_x}e^{nB_yh_y}ds\,dt\\
&=\iint_{N(P)}e^{n^2(B_xs+B_yt)+O(n)}\Big(\sum_{\{M\in\mathcal{M}(\mathsf{G}_n):h_x=\lfloor ns\rfloor,h_y=\lfloor nt\rfloor\}}\nu(M)\Big)ds\,dt\\
&=\iint_{N(P)}e^{n^2(B_xs+B_yt)+O(n)}e^{-n^2\sigma(s,t)+O(n)}ds\,dt,\quad\text{by definition of }\sigma(s,t)\\
&=\iint_{N(P)}e^{n^2(B_xs+B_yt-\sigma(s,t)+o(1))}ds\,dt.
\end{aligned}$$

An upper bound is obtained by writing:

$$\iint_{N(P)} e^{n^2(B_x s+B_y t-\sigma(s,t)+o(1))}\,ds\,dt \leq e^{n^2[\max_{\{(s,t)\in N(P)\}}(B_x s+B_y t-\sigma(s,t))+o(1)]}|N(P)|$$

A lower bound is obtained by performing Taylor expansion of $\phi(s,t) := B_x s + B_y t - \sigma(s,t)$ around its maximum and using the fact that the surface tension is strictly convex.

Taking $\frac{1}{n^2}\log$ yields that the Ronkin function is the Legendre transform of the surface tension:

$$R(B_x, B_y) = \max_{(s,t)\in N(P)} \{B_x s + B_y t - \sigma(s,t)\}.$$

□

Corollary 19. *The slope of the measure $\mu_{(B_x,B_y)}$ is the gradient of the Ronkin function at the point (B_x, B_y).*

3.4.3 Phases of the dimer model

In the introductory part of Section 3.4, we mentioned that a way to characterize phases of a given model is to use the rate of decay of edge-edge correlations and that, in the case of the dimer model, it required a characterization of the zeros of $P(e^{B_x}z, e^{B_y}w)$ on the unit torus. This information is now available and one can give a precise description of the phase diagram of the dimer model.

Actually, Kenyon, Okounkov and Sheffield use height function fluctuations to define the different phases, but show that this is equivalent to classifying phases using rate of decay of correlations. Here are their definitions:

- An EGM μ is called a *frozen phase* if there exists distinct faces f, f' of G for which $h(\mathsf{f})-h(\mathsf{f}')$ is deterministic.
- An EGM μ is called a *gaseous* or *smooth phase*, if the height fluctuations have bounded variance.
- An EGM μ is called a *liquid* or *rough phase*, if the μ-variance of the height difference is unbounded.

Now comes the theorem characterizing phases.

Theorem 20. [KOS06] *The measure $\mu_{(B_x,B_y)}$ is:*

- *frozen when (B_x, B_y) is in the closure of an unbounded connected component of the amoeba's complement $\mathbb{R}^2 \setminus \mathbb{A}(P)$,*
- *liquid when (B_x, B_y) is in the interior of the amoeba $\mathbb{A}(P)$,*
- *gaseous when (B_x, B_y) is in the closure of a bounded connected component of the amoeba's complement $\mathbb{R}^2 \setminus \mathbb{A}(P)$.*

Figure 3.9 represents the amoeba of the dimer model on the square-octagon graph with uniform weights, and the corresponding phases of the model.

We only give a few ideas on the proof of this theorem.

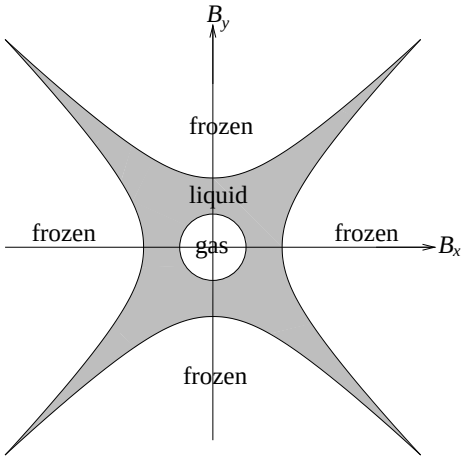

Figure 3.9: Phase diagram of the uniform dimer model on the square-octagon graph.

- Suppose that (B_x, B_y) is in the closure of an unbounded component of the amoeba's complement and recall (Corollary 19) that the slope of the measure $\mu_{(B_x,B_y)}$ is the gradient of the Ronkin function at the point (B_x, B_y). The slope is thus an integer point on the boundary of $N(P)$. Using the max-flow min cut theorem used by Thurston [Thu90] to give a criterion of existence of dimer configurations, one deduces that: if the slope is a non-extremal boundary point of $N(P)$, then there is an edge-path in the dual graph G_1^*, whose direction is orthogonal to the side of the Newton polygon, and such that dual edges crossing copies of this path appear with probability 1 or 0; if the slope is an extremal point of $N(P)$, there are two non-parallel edge-paths in the dual G_1^*, whose directions are orthogonal to the two side of the Newton polygon meeting at the extremal point, and such that dual edges crossing copies of these paths appear with probability 1 or 0. Otherwise stated, in the tiling representation of the dimer model, there are paths in the dual graph G_1^* generating a lattice of G^*, consisting of frozen paths for all tilings of G^* chosen with respect to the measure $\mu_{(B_x,B_y)}$. Tilings in connected components of the complement of this lattice are independent.

  The height difference of faces f, f' which belong to the lattice of frozen paths is constant, *i.e.* $h(\mathsf{f}) - h(\mathsf{f}')$ is deterministic and the measure $\mu_{(B_x,B_y)}$ is in the frozen phase.

In the other two cases, the proof consists of explicit asymptotic expansions of

$$K^{-1}_{(B_x,B_y)}(\mathsf{b}, \mathsf{w} + (x, y)),$$

which is the (x, y)-Fourier coefficient of $\frac{Q_{\mathsf{bw}}(e^{B_x} z, e^{B_y} w)}{P(e^{B_x} z, e^{B_y} w)}$ seen as a function of $(z, w) \in \mathbb{T}^2$.

- When (B_x, B_y) is in the interior of the amoeba, then $P(e^{B_x} z, e^{B_y} w)$ has 1 or 2 zeros on the unit torus, and KOS show that the only contribution to the (x, y)-Fourier coefficient comes from a neighborhood of the pole(s). They extract the exact asymptotics by doing Taylor approximations and contour integration, and show that $K^{-1}_{(B_x,B_y)}(\mathsf{b}, \mathsf{w} + (x, y))$ decreases linearly, implying that the edge covariances decreases quadratically. The authors then prove that the height difference between two faces f, f' grows universally like $\frac{1}{\pi}$ times the logarithm of the distance from f to f'. The measure $\mu_{(B_x,B_y)}$ is thus a liquid phase.

- When (B_x, B_y) belongs to the complement of the amoeba, then $P(e^{B_x}z, e^{B_y}w)$ has no zero on the unit torus, and $\frac{Q_{\mathsf{bw}}(e^{B_x}z, e^{B_y}w)}{P(e^{B_x}z, e^{B_y}w)}$ is analytic, implying that its Fourier coefficients decrease exponentially fast. When, (B_x, B_y) is in an unbounded component, then using the above specific argument of the frozen phase, the authors show that some Fourier coefficients are 0. When (B_x, B_y) is in a bounded component, then the Fourier coefficient decreases exponentially fast, and the height fluctuations have bounded variance. The measure $\mu_{(B_x,B_y)}$ is thus a gaseous phase.

3.5 Fluctuations of the height function

In this section we address the question of the fluctuations of the height function around its mean. We restrict ourselves to the case of the uniform dimer model on the infinite honeycomb lattice $\mathbb{H}$, with no magnetic field. The goal is to prove that the limiting fluctuations of the height function are described by a Gaussian free field of the plane, a behavior which is characteristic of the liquid phase.

Results presented here, and extensions can be found in [Ken00, Ken01, Ken08, dT07].

3.5.1 Uniform dimer model on the honeycomb lattice

Let us specify the results obtained in the previous sections to the case where $\mathbb{H}$ is the honeycomb lattice, edges are assigned weights 1, and there is no magnetic field. The choice of fundamental domain is given in Figure 3.10.

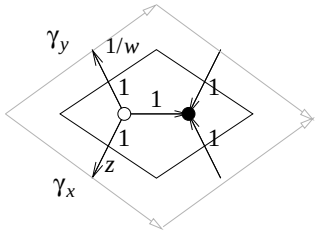

Figure 3.10: Choice of fundamental domain of the honeycomb lattice

The characteristic polynomial is:

$$P(z, w) = 1 + z + \frac{1}{w}.$$

The Gibbs measure μ obtained as weak limit of the Boltzmann measures μ_n on $\mathcal{M}(\mathsf{G}_n)$ (with no magnetic field) has the following expression on cylinder sets:

$$\mu(\mathsf{e}_1, \dots, \mathsf{e}_k) = \det\left(K^{-1}(\mathsf{b}_i, \mathsf{w}_j)_{1\leq i,j\leq k}\right), \tag{3.10}$$

where

$$K^{-1}(\mathsf{b}_{0,0}, \mathsf{w}_{x,y}) = \frac{1}{(2\pi i)^2}\int_{\mathbb{T}^2} \frac{1}{1 + z + \frac{1}{w}} z^y w^{-x} \frac{dz}{z}\frac{dw}{w},$$

and $\mathsf{w}_{x,y}$ represents the white vertex of the (x, y) copy of the fundamental domain, and similarly for $\mathsf{b}_{x,y}$.

When there is no magnetic field, the characteristic polynomial has two conjugate simple zeros on the unit torus $\mathbb{T}$: $(z_0, w_0) = (e^{i\frac{2\pi}{3}}, e^{i\frac{2\pi}{3}})$, and $(\overline{z_0}, \overline{w_0})$. The uniform dimer model on the honeycomb lattice is thus in the liquid phase.

In Section 2.4, we defined Thurston's height function on lozenge tilings of the triangular lattice $\mathbb{T}$, which was a function on vertices of $\mathbb{T}$. Equivalently, it is a function on dimer configurations of the honeycomb lattice $\mathbb{H}$, defined on faces of $\mathbb{H}$. For convenience, from now on, we consider $\frac{1}{3}$ of Thurston's height function.

The following lemma gives an expression of the height function using indicator functions of edges. We will use this in the proof of the convergence of the height function. Let u, v be two faces of $\mathbb{H}$, and let γ be an edge-path in the dual graph from u to v. Denote by $\mathsf{e}_1, \dots, \mathsf{e}_m$ the dual edges of edges of γ which have a black vertex on the left, and by $\mathsf{f}_1, \dots, \mathsf{f}_n$ those which have a white vertex on the left. Then,

Lemma 21.

$$h(\mathsf{v}) - h(\mathsf{u}) = \sum_{i=1}^{m} \left(-\mathbb{I}_{\mathsf{e}_i} + \frac{1}{3} \right) + \sum_{j=1}^{n} \left(\mathbb{I}_{\mathsf{f}_j} - \frac{1}{3} \right).$$

Proof. Let e_i be the dual edge of an edge $\mathsf{u}_i\mathsf{v}_i$ of γ, which has a black vertex on the left of γ. Then, returning to the orientation of the edges of the triangular lattice introduced in the construction of Thurston's height function, see Section 2.4, we know that the edge $\mathsf{u}_i\mathsf{v}_i$ is oriented from u_i to v_i. Thus by definition, we have:

$$h(\mathsf{v}_i) - h(\mathsf{u}_i) = \begin{cases} \frac{1}{3} & \text{if the edge } \mathsf{e}_i \text{ is not in the dimer configuration} \\ -\frac{2}{3} & \text{if the edge } \mathsf{e}_i \text{ is in the dimer configuration.} \end{cases}$$

This can be summarized as: $h(\mathsf{v}_i) - h(\mathsf{u}_i) = -\mathbb{I}_{\mathsf{e}_i} + \frac{1}{3}$.

A similar argument holds for edges which have a white vertex on the left. Summing over all edges in the path γ yields the result. □

3.5.2 Gaussian free field of the plane

We now define the Gaussian free field of the plane, which is, as we will see, the limiting object of the height function.

The *Green's function of the plane*, denoted by g satisfies $\Delta_x g(x, y) = \delta_x(y)$, where δ_x is the Dirac distribution at x. Up to an additive constant, g is given by

$$g(x, y) = -\frac{1}{2\pi} \log |x - y|.$$

Let $C^\infty_{c,0}(\mathbb{R}^2)$ be the set of C^∞ function of $\mathbb{R}^2$ with compact support and zero mean, and define the following continuous, bilinear form:

$$\begin{array}{rccl} G: & C^\infty_{c,0}(\mathbb{R}^2) \times C^\infty_{c,0}(\mathbb{R}^2) & \to & \mathbb{R} \\ & (\varphi_1, \varphi_2) & \mapsto & G(\varphi_1, \varphi_2) = \displaystyle\int_{\mathbb{R}^2} \int_{\mathbb{R}^2} g(x, y) \varphi_1(x) \varphi_2(y) dx\, dy. \end{array}$$

Introducing $f_i(x) = \sqrt{2} \int_{\mathbb{R}} g(x, y) \varphi_i(x) dx$, $i \in \{1, 2\}$, and using Green's formula, one shows that:

$$G(\varphi_1, \varphi_2) = \frac{1}{2} \int_{\mathbb{R}^2} \nabla f_1(x) \cdot \nabla f_2(x) dx,$$

implying that the bilinear form G is positive definite. The quantity $G(\varphi_1, \varphi_1)$ is known as the *Dirichlet energy* of f_1.

A *random generalized function* F assigns to every test function φ in $C^\infty_{c,0}(\mathbb{R}^2)$, a real random variable $F\varphi$. It is assumed to be linear and continuous, where continuity means that convergence of the functions φ_{n_j} $(1 \le j \le k)$ to φ_j, implies convergence in law of the random vector $(F\varphi_{n_1}, \dots, F\varphi_{n_k})$ to $(F\varphi_1, \dots, F\varphi_k)$. A *random generalized function* is said to be *Gaussian* if for every linearly independent functions $\varphi_1, \dots, \varphi_k \in C^\infty_{c,0}(\mathbb{R}^2)$, the random vector $(F\varphi_1, \dots, F\varphi_k)$ is Gaussian.

Theorem 22. [Boc55] *If $B : C^\infty_{c,0}(\mathbb{R}^2) \times C^\infty_{c,0}(\mathbb{R}^2) \to \mathbb{R}$ is a bilinear, continuous, positive definite form, then there exists a Gaussian random generalized function F, whose covariance function is given by:*

$$\mathbb{E}[F\varphi_1 F\varphi_2] = B(\varphi_1, \varphi_2).$$

By definition a *Gaussian free field of the plane* GFF is a Gaussian random generalized function whose covariance function is the bilinear form G defined above, *i.e.*

$$\mathbb{E}[\mathrm{GFF}(\varphi_1)\mathrm{GFF}(\varphi_2)] = -\frac{1}{2\pi}\int_{\mathbb{R}^2}\int_{\mathbb{R}^2} \log|x-y|\varphi_1(x)\varphi_2(y)dx\,dy.$$

There are other ways of defining the Gaussian free field, see for example [GJ81] and [She07].

3.5.3 Convergence of the height function to a Gaussian free field

Let $\mathbb{H}^\varepsilon$ be the graph $\mathbb{H}$ whose edge-lengths have been multiplied by ε, and consider the unnormalized height function h on faces of $\mathbb{H}^\varepsilon$. Define,

$$\begin{array}{rccl} H^\varepsilon : & C^\infty_{c,0}(\mathbb{R}^2) & \to & \mathbb{R} \\ & \varphi & \mapsto & H^\varepsilon\varphi = \varepsilon^2 \displaystyle\sum_{\mathsf{v}\in F(\mathbb{H}^\varepsilon)} \varphi(\mathsf{v})h(\mathsf{v}). \end{array}$$

Theorem 23. *The random generalized function H^ε converges weakly in law to $\frac{1}{\sqrt{\pi}}$ times a Gaussian free field,* i.e. *for every $\varphi_1, \dots, \varphi_k \in C^\infty_{c,0}(\mathbb{R}^2)$, $(H^\varepsilon\varphi_1, \dots, H^\varepsilon\varphi_k)$ converges in law (as $\varepsilon \to 0$) to $\frac{1}{\sqrt{\pi}}(\mathrm{GFF}\varphi_1, \dots, \mathrm{GFF}\varphi_k)$, where* GFF *is a Gaussian free field.*

Since the vector $(\mathrm{GFF}\varphi_1, \dots, \mathrm{GFF}\varphi_k)$ is Gaussian, to prove convergence of $(H^\varepsilon\varphi_1, \dots, H^\varepsilon\varphi_k)$ to $(\mathrm{GFF}\varphi_1, \dots, \mathrm{GFF}\varphi_k)$, it suffices to prove convergence of the moments of $(H^\varepsilon\varphi_1, \dots, H^\varepsilon\varphi_k)$ to those of $(\mathrm{GFF}\varphi_1, \dots, \mathrm{GFF}\varphi_k)$; that is we need to show that for every k-tuple of positive integers $(m_1, \dots, m_k)$, we have:

$$\lim_{\varepsilon\to 0} \mathbb{E}[(H^\varepsilon\varphi_1)^{m_1} \dots (H^\varepsilon\varphi_k)^{m_k}] = \mathbb{E}[(\mathrm{GFF}\varphi_1)^{m_1} \dots (\mathrm{GFF}\varphi_k)^{m_k}]. \tag{3.11}$$

We now state the key proposition used to prove convergence of the moments. Let $\mathsf{u}_1, \dots \mathsf{u}_k$, $\mathsf{v}_1, \dots, \mathsf{v}_k$ be distinct points of $\mathbb{R}^2$, and let $\gamma_1 \dots, \gamma_k$ be pairwise disjoint paths such that γ_j runs from u_j to v_j. Let $\mathsf{u}_j^\varepsilon, \mathsf{v}_j^\varepsilon$ be faces of $\mathbb{H}^\varepsilon$ lying within $O(\varepsilon)$ of u_j and v_j respectively. Then,

Proposition 24.

$$\lim_{\varepsilon\to 0} \mathbb{E}\left[(h(\mathsf{v}_1^\varepsilon) - h(\mathsf{u}_1^\varepsilon)) \dots (h(\mathsf{v}_k^\varepsilon) - h(\mathsf{u}_k^\varepsilon))\right] =$$

$$= \begin{cases} 0 & \text{when } k \text{ is odd} \\ \left(\dfrac{1}{\pi}\right)^{\frac{k}{2}} \displaystyle\sum_\sigma g(\mathsf{u}_{\sigma(1)}, \mathsf{v}_{\sigma(1)}, \mathsf{u}_{\sigma(2)}, \mathsf{v}_{\sigma(2)}) \dots g(\mathsf{u}_{\sigma(k-1)}, \mathsf{v}_{\sigma(k-1)}, \mathsf{u}_{\sigma(k)}, \mathsf{v}_{\sigma(k)}) & \text{when } k \text{ is even} \end{cases}$$

where $g(\mathsf{u},\mathsf{v},\mathsf{u}',\mathsf{v}') = g(\mathsf{v},\mathsf{v}') + g(\mathsf{u},\mathsf{u}') - g(\mathsf{v},\mathsf{u}') - g(\mathsf{u},\mathsf{v}')$, *$g$ is the Green's function of the plane, and the sum is over all* $(k-1)!!$ *pairings of* $\{1,\dots,k\}$.

Proof. We prove this proposition in a particular case. The proof of the general case is similar, although notationally much more cumbersome. Let us assume that $k = 2$, and suppose that $\mathsf{u}_1, \mathsf{v}_1, \mathsf{u}_2, \mathsf{v}_2$ are such that we can choose $\mathsf{u}_1^\varepsilon, \mathsf{v}_1^\varepsilon, \mathsf{u}_2^\varepsilon, \mathsf{v}_2^\varepsilon$ as in Figure 3.11. Let γ_1^ε and γ_2^ε be the paths joining $\mathsf{u}_1^\varepsilon, \mathsf{v}_1^\varepsilon$ and $\mathsf{u}_2^\varepsilon, \mathsf{v}_2^\varepsilon$ respectively as in Figure 3.11.

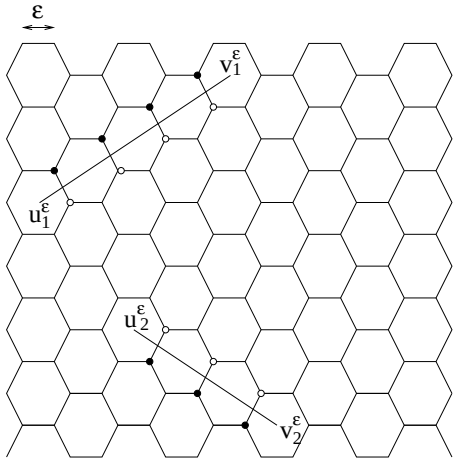

Figure 3.11: Choice of $\mathsf{u}_1^\varepsilon, \mathsf{u}_2^\varepsilon, \mathsf{v}_1^\varepsilon, \mathsf{v}_2^\varepsilon$

.

Denote by $\mathsf{e}_1 = \mathsf{w}_1\mathsf{b}_1, \dots, \mathsf{e}_m = \mathsf{w}_m\mathsf{b}_m$ the dual edges of the edges of the path γ_1^ε, and by $\mathsf{f}_1 = \mathsf{w}_1'\mathsf{b}_1', \dots, \mathsf{f}_n = \mathsf{w}_n'\mathsf{b}_n'$, the dual edges of the edges of γ_2^ε. Then, by Lemma 21,

$$\begin{aligned}
\mathbb{E}\left[(h(\mathsf{v}_1^\varepsilon) - h(\mathsf{u}_1^\varepsilon))(h(\mathsf{v}_2^\varepsilon) - h(\mathsf{u}_2^\varepsilon))\right] &= \mathbb{E}\left[\sum_{i=1}^m \left(-\mathbb{I}_{\mathsf{e}_i} + \frac{1}{3}\right) \sum_{j=1}^n \left(\mathbb{I}_{\mathsf{f}_j} - \frac{1}{3}\right)\right] \\
&= \sum_{i=1}^m \sum_{j=1}^n \left(-\mu(\mathsf{e}_i, \mathsf{f}_j) + \frac{1}{3}\mu(\mathsf{e}_i) + \frac{1}{3}\mu(\mathsf{f}_j) - \frac{1}{9}\right) \\
&= \sum_{i=1}^m \sum_{j=1}^n \left(-\mu(\mathsf{e}_i, \mathsf{f}_j) + \frac{1}{9}\right), \text{ (since } \mu(\mathsf{e}) = \frac{1}{3} \text{ for every edge } \mathsf{e}), \\
&= -\sum_{i=1}^m \sum_{j=1}^n K^{-1}(\mathsf{b}_i, \mathsf{w}_j') K^{-1}(\mathsf{b}_j', \mathsf{w}_i), \text{ (since } K(\mathsf{w}_i, \mathsf{b}_i) = K(\mathsf{w}_j', \mathsf{b}_j') = 1),
\end{aligned}$$

Using asymptotic formulae for $K^{-1}(\mathsf{b}_i, \mathsf{w}_j')$, $K^{-1}(\mathsf{b}_j', \mathsf{w}_i)$ (see either [KOS06] or [Ken02]), one obtains:

$$-K^{-1}(\mathsf{b}_i, \mathsf{w}_j')K^{-1}(\mathsf{b}_j', \mathsf{w}_i) = -\frac{1}{(2\pi)^2}\left(\frac{\varepsilon^2 dz_j' dz_i}{(z_j' - z_i)^2} + \frac{\varepsilon^2 d\bar{z}_j' d\bar{z}_i}{(\bar{z}_j' - \bar{z}_i)^2}\right) + \text{ cross terms} + o(),$$

where z_j' and z_i are points approximating w_j', b_j' and $\mathsf{w}_i, \mathsf{b}_i$, respectively. One can show that the sum over the paths γ_1^ε, γ_2^ε of the cross terms is $O(\varepsilon)$, so that summing over all edges in the paths

yields:

$$\begin{aligned}\lim_{\varepsilon\to 0}\mathbb{E}\left[(h(\mathsf{v}_1^\varepsilon)-h(\mathsf{u}_1^\varepsilon))(h(\mathsf{v}_2^\varepsilon)-h(\mathsf{u}_2^\varepsilon))\right] &= -2\,Re\int_{\mathsf{u}_1}^{\mathsf{v}_1}\int_{\mathsf{u}_2}^{\mathsf{v}_2}\frac{1}{4\pi^2(z_2-z_1)^2}dz_1dz_2\\ &= -\frac{1}{2\pi^2}\log\left|\frac{(\mathsf{v}_1-\mathsf{v}_2)(\mathsf{u}_1-\mathsf{u}_2)}{(\mathsf{v}_1-\mathsf{u}_2)(\mathsf{u}_1-\mathsf{v}_2)}\right|\\ &= \frac{1}{\pi}g(\mathsf{u}_1,\mathsf{v}_1,\mathsf{u}_2,\mathsf{v}_2).\end{aligned}$$

□

Once Proposition 24 is available, one then introduces test functions and prove convergence of all moments of (3.11). This implies handling moments of height differences involving vertices which are close. The asymptotic formula for the inverse Kasteleyn matrix does not hold in this case, and one has to do careful bounds to see that everything still works.

****

We have reached the end of these lecture notes covering the foundations of the dimer model and the paper "Dimers and amoeba" of Kenyon, Okounkov and Sheffield [KOS06], giving a full description of the phase diagram of the dimer model on periodic, bipartite graphs. Although these are spectacular results, there are others, such as the specific behavior of the dimer model defined on isoradial graphs [Ken02, KO06], the understanding of limit shapes [CKP01, KO07], the application of dimer techniques to study the Ising model [BdT10b, BdT10a]. We do hope that these notes will encourage the reader to learn more on this very rich model of statistical mechanics.

Bibliography

[Bax89] Rodney J. Baxter. *Exactly solved models in statistical mechanics*. Academic Press Inc. [Harcourt Brace Jovanovich Publishers], London, 1989. Reprint of the 1982 original.

[BdT10a] Cédric Boutillier and Béatrice de Tilière. The critical Z-invariant Ising model via dimers: locality property. *Comm. Math. Phys.*, pages 1–44, 2010.

[BdT10b] Cédric Boutillier and Béatrice de Tilière. The critical Z-invariant Ising model via dimers: the periodic case. *Probab. Theory Related Fields*, 147:379–413, 2010.

[Boc55] S. Bochner. *Harmonic analysis and the theory of probability*. University of California press, 1955.

[BR06] B. Bollobás and O. Riordan. *Percolation*. Cambridge Univ Pr, 2006.

[CKP01] Henry Cohn, Richard Kenyon, and James Propp. A variational principle for domino tilings. *J. Amer. Math. Soc.*, 14(2):297–346 (electronic), 2001.

[CR07] David Cimasoni and Nicolai Reshetikhin. Dimers on surface graphs and spin structures. I. *Comm. Math. Phys.*, 275(1):187–208, 2007.

[CR08] David Cimasoni and Nicolai Reshetikhin. Dimers on surface graphs and spin structures. II. *Comm. Math. Phys.*, 281(2):445–468, 2008.

[CS12] D. Chelkak and S. Smirnov. Universality in the 2D Ising model and conformal invariance of fermionic observable. *Invent. Math.*, 189:515–580, 2012.

[DS11] B. Duplantier and S. Sheffield. Liouville quantum gravity and KPZ. *Invent. Math.*, 185(2):333–393, 2011.

[DT89] G. David and C. Tomei. The problem of Calissons. *Amer. Math. Monthly*, 96(5):429–431, 1989.

[dT07] B. de Tilière. Scaling limit of isoradial dimer models and the case of triangular quadri-tilings. *Ann. Inst. Henri Poincaré (B) Probab. Stat.*, 43(6):729–750, 2007.

[DZM+96] N. P. Dolbilin, Yu. M. Zinov′ev, A. S. Mishchenko, M. A. Shtan′ko, and M. I. Shtogrin. Homological properties of two-dimensional coverings of lattices on surfaces. *Funktsional. Anal. i Prilozhen.*, 30(3):19–33, 95, 1996.

[FPT00] M. Forsberg, M. Passare, and A. Tsikh. Laurent determinants and arrangements of hyperplane amoebas. *Adv. Math.*, 151(1):45–70, 2000.

[FR37] RH Fowler and GS Rushbrooke. An attempt to extend the statistical theory of perfect solutions. *Transactions of the Faraday Society*, 33:1272–1294, 1937.

[GJ81] J. Glimm and A. Jaffe. *Quantum physics: a functional integral point of view.* Springer-Verlag, 1981.

[GKZ94] I.M. Gelfand, M.M. Kapranov, and A.V. Zelevinsky. *Discriminants, resultants, and multidimensional determinants.* Springer, 1994.

[GL99] A. Galluccio and M. Loebl. On the theory of Pfaffian orientations. I. Perfect matchings and permanents. *Electron. J. Combin.*, 6(1):R6, 1999.

[Gri99] G. Grimmett. *Percolation.* Springer Verlag, 1999.

[HJ90] R.A. Horn and C.R. Johnson. *Matrix analysis.* Cambridge University Press, 1990.

[Kas61] P. W. Kasteleyn. The statistics of dimers on a lattice : I. The number of dimer arrangements on a quadratic lattice. *Physica*, 27:1209–1225, Dec 1961.

[Kas67] P. W. Kasteleyn. Graph theory and crystal physics. In *Graph Theory and Theoretical Physics*, pages 43–110. Academic Press, London, 1967.

[Ken] R. Kenyon. Lectures on dimers, statistical mechanics. *IAS/Park City Math. Ser*, 16:191–230.

[Ken97] Richard Kenyon. Local statistics of lattice dimers. *Ann. Inst. Henri Poincaré Probab. Stat.*, 33(5):591–618, 1997.

[Ken00] R. Kenyon. Conformal invariance of domino tiling. *Ann. Probab.*, 28(2):759–795, 2000.

[Ken01] R. Kenyon. Dominos and the Gaussian free field. *Ann. Probab.*, 29(3):1128–1137, 2001.

[Ken02] Richard Kenyon. The Laplacian and Dirac operators on critical planar graphs. *Invent. Math.*, 150(2):409–439, 2002.

[Ken04] Richard Kenyon. An introduction to the dimer model. In *School and Conference on Probability Theory*, pages 267–304. ICTP Lect. Notes, XVII, Abdus Salam Int. Cent. Theoret. Phys., Trieste, 2004.

[Ken08] R. Kenyon. Height fluctuations in the honeycomb dimer model. *Comm. Math. Phys.*, 281(3):675–709, 2008.

[Kes82] H. Kesten. *Percolation theory for mathematicians.* Birkhäuser, 1982.

[KO06] Richard Kenyon and Andrei Okounkov. Planar dimers and Harnack curves. *Duke Math. J.*, 131(3):499–524, 2006.

[KO07] R. Kenyon and A. Okounkov. Limit shapes and the complex Burgers equation. *Acta Math.*, 199(2):263–302, 2007.

[KOS06] Richard Kenyon, Andrei Okounkov, and Scott Sheffield. Dimers and amoebae. *Ann. of Math. (2)*, 163(3):1019–1056, 2006.

[KPW00] R.W. Kenyon, J.G. Propp, and D.B. Wilson. Trees and matchings. *Electron. J. Combin*, 7(1):R25, 2000.

[Kup98] Greg Kuperberg. An exploration of the permanent-determinant method. *Electron. J. Combin.*, 5:Research Paper 46, 34 pp. (electronic), 1998.

[LSW04] G.F. Lawler, O. Schramm, and W. Werner. Conformal invariance of planar loop-erased random walks and uniform spanning trees. *Ann. Probab.*, 32(1):939–995, 2004.

[Mac01] P.A. MacMahon. *Combinatory analysis*. Chelsea Pub Co, 2001.

[Mik00] G. Mikhalkin. Real algebraic curves, the moment map and amoebas. *Ann. of Math. (2)*, 151(1):309–326, 2000.

[MR01] G. Mikhalkin and H. Rullgård. Amoebas of maximal area. *Int. Math. Res. Not.*, 2001(9):441, 2001.

[MW73] B. McCoy and F. Wu. *The two-dimensional Ising model*. Harvard Univ. Press, 1973.

[Ons44] Lars Onsager. Crystal statistics. I. A two-dimensional model with an order-disorder transition. *Phys. Rev.*, 65(3-4):117–149, Feb 1944.

[Per69] J.K. Percus. One more technique for the dimer problem. *J. Math. Phys.*, 10:1881, 1969.

[Sch00] O. Schramm. Scaling limits of loop-erased random walks and uniform spanning trees. *Israel J. Math.*, 118(1):221–288, 2000.

[She05] Scott Sheffield. Random surfaces. *Astérisque*, (304):vi+175, 2005.

[She07] S. Sheffield. Gaussian free fields for mathematicians. *Probab. Theory Related Fields*, 139(3):521–541, 2007.

[Smi10] S. Smirnov. Conformal invariance in random cluster models. I. Holomorphic fermions in the Ising model. *Ann. of Math. (2)*, 172(2):1435–1467, 2010.

[Sos07] A. Soshnikov. Determinantal random point fields. *Russian Mathematical Surveys*, 55(5):923, 2007.

[Tes00] G. Tesler. Matchings in graphs on non-orientable surfaces. *J. Combin. Theory Ser. B*, 78(2):198–231, 2000.

[TF61] HNV Temperley and M.E. Fisher. Dimer problem in statistical mechanics-an exact result. *Philosophical Magazine*, 6(68):1061–1063, 1961.

[Thu90] W.P. Thurston. Conway's tiling groups. *Amer. Math. Monthly*, 97(8):757–773, 1990.

[Vel] Y. Velenik. Le modèle d'Ising. *http://www.unige.ch/math/folks/velenik/cours.html.*

[W+07] W. Werner et al. Lectures on two-dimensional critical percolation. *Arxiv*, 0710.0856, 2007.

[Wer09] W. Werner. Percolation et modèle d'Ising. *Cours spécialisés, SMF*, 16, 2009.